

เส้นใยนาโนของพอลิไวนิลแอลกอฮอล์อิเล็กโทรสปินแบบเรียงตัวสำหรับ
อัลตราทินแลร์โครมาโทกราฟี



นางสาวรัญญา อัคราศรี

จุฬาลงกรณ์มหาวิทยาลัย

CHULALONGKORN UNIVERSITY

บทคัดย่อและแฟ้มข้อมูลฉบับเต็มของวิทยานิพนธ์ตั้งแต่ปีการศึกษา 2554 ที่ให้บริการในคลังปัญญาจุฬาฯ (CUIR)
เป็นแฟ้มข้อมูลของนิสิตเจ้าของวิทยานิพนธ์ ที่ส่งผ่านทางบัณฑิตวิทยาลัย

The abstract and full text of theses from the academic year 2011 in Chulalongkorn University Intellectual Repository (CUIR)
are the thesis authors' files submitted through the University Graduate School.

วิทยานิพนธ์นี้เป็นส่วนหนึ่งของการศึกษาตามหลักสูตรปริญญาวิทยาศาสตรมหาบัณฑิต

สาขาวิชาปิโตรเคมีและวิทยาศาสตร์พอลิเมอร์

คณะวิทยาศาสตร์ จุฬาลงกรณ์มหาวิทยาลัย

ปีการศึกษา 2557

ลิขสิทธิ์ของจุฬาลงกรณ์มหาวิทยาลัย

ALIGNED ELECTROSPUN POLY(VINYL ALCOHOL) NANOFIBERS FOR ULTRATHIN
LAYER CHROMATOGRAPHY

Miss Waranya Akhahardsri



A Thesis Submitted in Partial Fulfillment of the Requirements
for the Degree of Master of Science Program in Petrochemistry and Polymer Science
Faculty of Science
Chulalongkorn University
Academic Year 2014
Copyright of Chulalongkorn University

Thesis Title	ALIGNED ELECTROSPUN POLY(VINYL ALCOHOL) NANOFIBERS FOR ULTRATHIN LAYER CHROMATOGRAPHY
By	Miss Waranya Akhahardsri
Field of Study	Petrochemistry and Polymer Science
Thesis Advisor	Puttaruksa Varanusupakul, Ph.D.

Accepted by the Faculty of Science, Chulalongkorn University in Partial
Fulfillment of the Requirements for the Master's Degree

.....Dean of the Faculty of Science
(Professor Supot Hannongbua, Dr.rer.nat.)

THESIS COMMITTEE

.....Chairman
(Assistant Professor Warinthorn Chavasiri, Ph.D.)

.....Thesis Advisor
(Puttaruksa Varanusupakul, Ph.D.)

.....Examiner
(Associate Professor Mongkol Sukwattanasinitt, Ph.D.)

.....External Examiner
(Tinnakorn Tiensing, Ph.D.)

วรัญญา อัครชาติศรี : เส้นใยนาโนของพอลิไวนิลแอลกอฮอล์อิเล็กโทรสปินแบบเรียงตัวสำหรับอัลตราทินแลร์โครมาโทกราฟี (ALIGNED ELECTROSPUN POLY(VINYL ALCOHOL) NANOFIBERS FOR ULTRATHIN LAYER CHROMATOGRAPHY) อ.ที่ปรึกษาวิทยานิพนธ์
 หลัก: ดร.พุทธิรักษา วรานุศุภากุล, 67 หน้า.

เส้นใยนาโนของพอลิไวนิลแอลกอฮอล์อิเล็กโทรสปินแบบเรียงตัวสามารถเตรียมได้ด้วยเทคนิคอิเล็กโทรสปินนิ่งและนำมาใช้เป็นเฟสคงที่สำหรับอัลตราทินแลร์โครมาโทกราฟี พอลิไวนิลแอลกอฮอล์สามารถละลายในน้ำได้จึงเป็นข้อจำกัดสำหรับการนำมาใช้เป็นเฟสคงที่ เพื่อเพิ่มความเสถียรในน้ำจึงต้องเชื่อมขวางพอลิไวนิลแอลกอฮอล์ด้วยกลูทารัลดีไฮด์เป็นเวลา 5 ชั่วโมง ก่อนกระบวนการอิเล็กโทรสปินนิ่ง เส้นใยนาโนของพอลิไวนิลแอลกอฮอล์อิเล็กโทรสปินแบบเรียงตัวสามารถเตรียมได้โดยสภาวะ ดังนี้ ศักย์ไฟฟ้า 24 กิโลโวลต์ อัตราการไหลของสารละลาย 7 ไมโครลิตรต่อนาที ระยะทางระหว่างตัวรองรับ 15 เซนติเมตร และตัวรองรับแบบแกนหมุน ที่มีความเร็วรอบ 1250 รอบต่อนาที ซึ่งได้เส้นใยที่มีลักษณะเส้นใยและการเรียงตัวของเส้นใยเป็นที่น่าพอใจ เส้นใยนาโนของพอลิไวนิลแอลกอฮอล์อิเล็กโทรสปินแบบเรียงตัวในสภาวะนี้จะมีขนาดเส้นผ่านศูนย์กลางเฉลี่ย 459 ± 71 นาโนเมตร และมีเส้นใยที่เรียงตัวและทำมุมน้อยกว่า 5 องศาจากเส้นอ้างอิง 65% สำหรับประสิทธิภาพในการแยก เฟสเคลื่อนที่จะเคลื่อนที่ผ่านแผ่นเส้นใยนาโนของพอลิไวนิลแอลกอฮอล์อิเล็กโทรสปินแบบเรียงตัวสอดคล้องกับสมการของลูคัส-วอชเบิร์ต ซึ่งแสดงว่าการเคลื่อนที่ของเฟสคงที่ในเส้นใยนาโนของพอลิไวนิลแอลกอฮอล์อิเล็กโทรสปินแบบเรียงตัวใช้แรงแคปิลารีผ่านตัวกลางซึ่งคล้ายกับซิลิกา นอกจากนี้การเคลื่อนที่ของเฟสเคลื่อนที่บนแผ่นเส้นใยนาโนของพอลิไวนิลแอลกอฮอล์อิเล็กโทรสปินแบบเรียงตัวจะเร็วกว่าแผ่นเส้นใยนาโนของพอลิไวนิลแอลกอฮอล์อิเล็กโทรสปินและแผ่นซิลิกา ซึ่งค่าคงที่ความเร็วในเส้นใยนาโนของพอลิไวนิลแอลกอฮอล์อิเล็กโทรสปินแบบเรียงตัว คือ 0.0985 ตารางเซนติเมตรต่อวินาที ซึ่งสูงกว่าเส้นใยนาโนของพอลิไวนิลแอลกอฮอล์อิเล็กโทรสปิน ซึ่งมีค่าคงที่ความเร็ว 0.0448 ตารางเซนติเมตรต่อวินาที ประมาณ 2 เท่าและสูงกว่าเส้นใยซิลิกา 6 เท่า ซึ่งมีค่าคงที่ความเร็ว 0.019 ตารางเซนติเมตรต่อวินาที สุดท้ายได้ทำการวิเคราะห์กรดอะมิโนด้วยแผ่นเส้นใยนาโนของพอลิไวนิลแอลกอฮอล์อิเล็กโทรสปินแบบเรียงตัวเปรียบเทียบกับเส้นใยนาโนของพอลิไวนิลแอลกอฮอล์อิเล็กโทรสปินและแผ่นซิลิกา โดยเปรียบเทียบประสิทธิภาพการแยกด้วยค่าจำนวนแผ่นและความสูงของแผ่น พบว่าแผ่นเส้นใยนาโนของพอลิไวนิลแอลกอฮอล์อิเล็กโทรสปินแบบเรียงตัวมีประสิทธิภาพน้อยกว่าแผ่นเส้นใยนาโนของพอลิไวนิลแอลกอฮอล์อิเล็กโทรสปิน เนื่องจากรูปร่างและขนาดของจุดสารตัวอย่าง อย่างไรก็ตาม เวลาที่ใช้ในการวิเคราะห์ด้วยแผ่นเส้นใยนาโนของพอลิไวนิลแอลกอฮอล์อิเล็กโทรสปินแบบเรียงตัวน้อยกว่าการวิเคราะห์ด้วยแผ่นเส้นใยนาโนของพอลิไวนิลแอลกอฮอล์อิเล็กโทรสปินและแผ่นซิลิกา 4-5 เท่า

สาขาวิชา ปีโตรเคมีและวิทยาศาสตร์พอลิเมอร์

ปีการศึกษา 2557

ลายมือชื่อนิสิต

ลายมือชื่อ อ.ที่ปรึกษาหลัก

5472092323 : MAJOR PETROCHEMISTRY AND POLYMER SCIENCE

KEYWORDS: ULTRATHIN LAYER CHROMATOGRAPHY / POLY(VINYL ALCOHOL) / ALIGNED ELECTROSPUN NANOFIBERS

WARANYA AKHAHARDSRI: ALIGNED ELECTROSPUN POLY(VINYL ALCOHOL) NANOFIBERS FOR ULTRATHIN LAYER CHROMATOGRAPHY. ADVISOR: PUTTARUKSA VARANUSUPAKUL, Ph.D., 67 pp.

Aligned electrospun poly(vinyl alcohol) nanofibers (AE-PVA) were fabricated by electrospinning technique and applied as a stationary phase for ultrathin layer chromatography (UTLC). Because PVA is soluble in water, this is a limitation for using AE-PVA as a stationary phase. To enhance the stability in water, PVA was crosslinked by glutaraldehyde for 5 h before electrospinning process. The AE-PVA nanofibers generated at the electrospinning condition as follow; high voltage of 24 kV, solution flow rate of 7 mL/min, collector distance of 15 cm and rotational speed of collector of 1250 rpm, provided the most satisfied nanofibers in term of morphology and alignment of fibers. The average diameter of AE-PVA fibers at this condition was 459 ± 71 nm and 65% of fibers were aligned within 5° angle from the virtual line. For separation performance, the mobile phase transport on the AE-PVA UTLC was fitted the Lucas-Washburn equation which was referred that the transport of mobile phase was mainly based on capillary flow through porous media similar to that on conventional silica TLC. Moreover, the migration of mobile phase on AE-PVA UTLC was more rapid than that on E-PVA UTLC and silica TLC as the velocity constant of AE-PVA UTLC was $0.0985 \text{ cm}^2/\text{s}$ which was twice higher than that of E-PVA which was $0.0448 \text{ cm}^2/\text{s}$ and 6 times higher than that of silica fibers UTLC which was $0.019 \text{ cm}^2/\text{s}$. Finally, the analysis of amino acids was performed using AE-PVA UTLC and compared to E-PVA UTLC and silica TLC. The separation efficiency of AE-PVA UTLC which was demonstrated by the plate number and plate height was comparable with silica TLC but less efficient than E-PVA which caused by shape and size of sample spot on the plate. However, the analysis time of AE-PVA UTLC was greatly decrease by the factor of 4-5 times comparing with E-PVA and silica TLC.

Field of Study: Petrochemistry and Polymer Student's Signature

Science Advisor's Signature

Academic Year: 2014

ACKNOWLEDGEMENTS

The author highly appreciates people who kindly support the knowledge of this study. Firstly, I would like to express sincere thanks to my advisor, Dr. Puttaruksa Varanusupakul for her useful instruction, continuous support, advance technique, encouragements and intensive proofreading throughout this research. This thesis would not been completed without all supports from her. Additionally, I am particularly grateful for Assistant Professor Dr. Warinthorn Chavasiri, Associate Professor Dr. Mongkol Sukwattanasinitt and Dr. Tinnakorn Tiensing who valuable suggestion for mythesis.

I would like to thanks many people in Chromatography and Separation Research Unit and members of 1205/1207 Laboratory especially Mr. Taweesak Chanduang who assist providing all equipment.

Finally, I appreciatively acknowledge my family and my friends for all their supports and encouragements throughout the period of this research.

CONTENTS

	Page
THAI ABSTRACT.....	iv
ENGLISH ABSTRACT	v
ACKNOWLEDGEMENTS.....	vi
CONTENTS	vii
LIST OF TABLES.....	x
LIST OF FIGURES.....	xi
LIST OF SCHEMES.....	xiv
LIST OF ABBREVIATION.....	xv
CHAPTER I INTRODUCTION.....	1
1.1 Statement of purpose	1
1.2 Objective of the research.....	3
1.3 Scopes of the research.....	3
1.4 Benefits of the research.....	3
CHAPTER II THEORY AND LITERATURE REVIEWS	4
2.1 Electrospinning.....	4
2.2 Parameters of electrospinning technique	6
2.2.1 The Solution properties	6
2.2.1.1 Concentration	6
2.2.1.2 Surface tension	7
2.2.1.3 Molecular weight	7
2.2.2 Processing conditions of electrospinning.....	9
2.2.2.1 Applied voltage.....	9

	Page
2.2.2.2 Distance between the tip of needle and collector or collector distance.....	10
2.2.2.3 Flow rate.....	11
2.2.2.4 Type of collector.....	11
2.2.3 Environmental conditions.....	14
2.3 Poly(vinyl alcohol) or PVA.....	16
2.4 Thin layer chromatography (TLC).....	17
2.5 High performance thin layer chromatography (HPTLC).....	19
2.6 Ultrathin layer chromatography (UTLC).....	20
2.6.1 Monolith.....	20
2.6.2 Nanostructure.....	20
2.6.3 Electrospun nanofibers.....	21
CHAPTER III EXPERIMENTAL.....	22
3.1 Chemicals and materials.....	22
3.2 Preparation of solution.....	23
3.2.1 Amino acid standard solutions.....	23
3.2.2 Ninhydrin solution.....	23
3.2.3 Developing solvent for TLC separation.....	23
3.3 Methodology.....	24
3.3.1 Preparation of aligned electrospun PVA nanofibers.....	24
3.3.2 Characterization of aligned electrospun nanofibers.....	26
3.3.2.1 Fourier Transform Infrared Spectroscopy (FT-IR).....	26
3.3.2.2 Scanning Electron Microscopy (SEM).....	26

	Page
3.3.2.3 Alignment of electrospun nanofibers	26
3.3.3 TLC separation.....	27
3.3.3.1 Velocity constant of mobile phase	27
3.3.3.2 Separation of amino acids.....	28
CHAPTER IV RESULTS AND DISCUSSION.....	29
4.1 Characterization of E-PVA and AE-PVA nanofibers by FTIR spectroscopy.....	30
4.2 Characterization of E-PVA and AE-PVA nanofibers by SEM.....	32
4.2.1 Effect of collector distance.....	33
4.2.2 Effect of rotational speed	33
4.3 Alignment of electrospun nanofibers.....	36
4.4 TLC Separation.....	40
4.4.1 Migration of mobile phase	40
4.4.2 Separation of amino acids.....	42
REFERENCES.....	56
APPENDIX.....	63
VITA.....	67

LIST OF TABLES

Table	Page
3.1 Solvent for preparing amino acid standard solutions.....	23
4.1 Average diameter of E-PVA and AE-PVA nanofibers.....	32
4.2 The velocity constant (K) of AE-PVA-UTLC plates.....	41
4.3 Analysis time, spot width, plate number (N), plate height (H) studied of amino acids for AE-PVA-UTLC, E-PVA-UTLC and silica TLC.....	48



LIST OF FIGURES

Figure	Page
2.1 (A) schematic of electrospinning process, (B) plate collector, (C) random electrospun nanofibers collecting on plate collector, (D) rotating collector, (E) aligned electrospun nanofibers collecting on rotating collector	4
2.2 Schematic of Taylor cone formation (A) hemispherical shape, (B) elongated polymer solution, (c) Taylor cone	5
2.3 Morphology of electrospun at various concentration of polystyrene solution (A) 2.5 wt%, (B) 4.8 wt%, (C) 13.1 wt%, (D) 20.2 wt%.....	6
2.4 TEM of 4 wt% of polyvinylpyrrolidone dissolved in (A) ethanol, (B) dichloromethane, (C) dimethylformamide.....	7
2.5 SEM images of 25 wt% PVA solution which various molecular weight (A) 9,000-10,000 g/mol, (B) 13,000-23,000 g/mol and (C) 31,000-50,000 g/mol.....	8
2.6 SEM images of the electrospun fibers from a 20 % polysulfone solution in N,N-dimethylacetamide/acetone. High voltage was applied at (a) 10 kV, (b) 15 kV and (c) 20 kV	9
2.7 SEM images of PVA 10% w/v of PVA solution which collector distance was (A) 5 cm, (B) 10 cm, (C) 15 cm, (D) 20 cm.....	10
2.8 Plate collector and electrospun nanofibers	11
2.9 Rotating drum.....	12
2.10 Rotational speed of (A) 350 rpm, (B) 4500 rpm, (C) 6000 rpm, (D) 7500 rpm....	13
2.11 Disc collector.....	14
2.12 polystyrene electrospun nanofibers under different humidity (a) <25%, (b) 31-38%, (c) 40-45%, (d) 50-59%, (e) 60-72% RH	15
2.13 TLC plate development.....	17

Figure	Page
2.14 SEM image of macroporous GLAD thin film (A and B) isotropic, (C and D) anisotropic and (E and F) blade-like.....	21
3.1 Electrospinning process setup.....	25
4.1 FT-IR spectra of PVA and crosslinked PVA nanofibers (a) PVA, (b) E-PVA, (c) AE-PVA at 500 rpm, (d) AE-PVA at 750 rpm, (e) AE-PVA at 1000 rpm, (f) AE-PVA at 1250 rpm and (g) AE-PVA at 1500 rpm.....	31
4.2 SEM images illustrating E-PVA and AE-PVA nanofibers generated on the collector distance of 15 cm. (A) E-PVA (B) AE-PVA at 500 rpm, (C) AE-PVA at 750 rpm, (D) AE-PVA at 1000 rpm, (E) AE-PVA at 1250 rpm and (F) AE-PVA at 1500 rpm.	34
4.3 SEM images illustrating E-PVA and AE-PVA nanofibers generated on the collector distance of 20 cm. (A) E-PVA (B) AE-PVA at 500 rpm, (C) AE-PVA at 750 rpm, (D) AE-PVA at 1000 rpm, (E) AE-PVA at 1250 rpm and (F) AE-PVA at 1500 rpm.	35
4.4 SEM images illustrating AE-PVA nanofibers generated on the rotating collector at rotational speeds of (A) 500 rpm, (B) 750 rpm, (C) 1000 rpm, (D)1250 rpm and (E) 1500 rpm. The collector distance was 15 cm. The white line represents the virtual line of alignment of nanofibers.....	37
4.5 SEM images illustrating AE-PVA nanofibers generated on the rotating collector at rotational speeds of (A) 500 rpm, (B) 750 rpm, (C) 1000 rpm, (D)1250 rpm and (E) 1500 rpm. The collector distance was 20 cm. The white line represents the virtual line of alignment of nanofibers.....	38
4.6 Percentage of AE-PVA fibers positioned in range of below 5° , $5^\circ - 10^\circ$, $10^\circ - 15^\circ$ and above 15° angle from the virtual line. (collector distance : 15 cm) ..	39
4.7 Percentage of AE-PVA fibers positioned in range of below 5° , $5^\circ - 10^\circ$, $10^\circ - 15^\circ$ and above 15° angle from the virtual line. (collector distance : 20 cm) ..	39

Figure	Page
4.8 Comparison of velocity constants of mobile phase AE-PVA UTLC at rotational speed of 1250 rpm and silica TLC.....	40
4.9 Structure of alanine, glutamine, methionine, phenylalanine and threonine....	42
4.10 The analysis of amino acids on the AE-PVA-UTLC at 1250 rpm.....	43
4.11 The analysis of amino acids on the E-PVA-UTLC.....	44
4.12 The analysis of amino acids on the silica TLC.....	45
4.13 R_f of amino acids on E-PVA-UTLC, AE-PVA-UTLC and Silica TLC plate.....	46
4.14 The original spot of silica TLC, E-PVA-UTLC and AE-PVA-UTLC.....	47
4.15 The separation of Met and Phe on the silica TLC, E-PVA-UTLC and AE-PVA-UTLC.....	50
4.16 The separation of Met and Ala on the silica TLC, E-PVA-UTLC and AE-PVA-UTLC.....	51
4.17 The separation of Met and Gln on the silica TLC, E-PVA-UTLC and AE-PVA-UTLC.....	52
4.18 The separation of Ala and Gln on the silica TLC, E-PVA-UTLC and AE-PVA-UTLC.....	53

LIST OF SCHEMES

Scheme	Page
4.1 The reaction of crosslinked PVA.....	29



LIST OF ABBREVIATION

AE-PVA	Aligned electrospun poly(vinyl alcohol)
Ala	Alanine
cm	Centimeter
°C	Degree Celsius
E-PVA	Electrospun poly(vinyl alcohol)
FT-IR	Fourier Transform Infrared Spectroscopy
GA	Glutaraldehyde
Gln	Glutamine
HPTLC	High performance thin layer chromatography
h	Hour
kV	Kilovolt
Met	Methionine
µg	Microgram
µL	Microliter
mg	Milligram
mL	Milliliter
min	Minute
nL	Nanoliter
nm	Nanometer
Phe	Phenylalanine
rpm	Round per minute
sec	second
SEM	Scanning Electron Microscopy
Thr	Threonine
TLC	Thin layer chromatography
UTLC	Ultrathin layer chromatography
wt%	Weight percentage

CHAPTER I

INTRODUCTION

1.1 Statement of purpose

Thin layer chromatography (TLC) is a planar chromatography and was introduced in the 1950s. TLC is used to separate compounds in mixture. The benefits of TLC are simple, efficient, low cost and fast process. TLC is used in many fields such as pharmaceutical, environmental, food, herbal medicinal, forensic and clinical science as well as toxicology and quality control [1-4]. Normally, TLC technique performs on a support plate coated with a thin layer of solid particles of stationary phase or sometimes called sorbent. Silica, alumina, kieselguhr, magnesium silicate and magnesium oxide are used as stationary phase [5]. The particle size of sorbent in TLC is generally 10-12 μm with the thickness of 100-400 μm . The support plates are made by inert material such as glass, aluminium or terephthalate foil, poly tetrafluoroethylene (PTFE) and glass fiber. Usually, binder was added to enhance the attachment of solid particles on the support plate.

Because a higher efficiency and better resolution can be resulted from reducing the particle size and a thickness of layer of stationary phase, high-performance thin layer chromatography (HPTLC) and ultrathin layer chromatography (UTLC) were developed and introduced in the 1970s and 2001, respectively. HPTLC consists of the particle size of stationary phase in range of 4-6 μm and the thickness of 100-200 μm [3] while UTLC uses the nanomaterials as stationary phase and the thickness of 5-25 μm . Several materials, for example, monolith [6, 7], nanofibers which were prepared by electrospinning technique [4, 8], and a porous nanostructure which was prepared by the glancing-angle deposition (GLAD) [6, 9, 10] were applied as the stationary phase in UTLC. Comparing UTLC to HPTLC, UTLC shows the advantages of

shorter analysis time, less material consumption, higher sensitivity and lower detection limit [11].

Many researchers were studied and reported the application of nanofibers generated by electrospinning technique as the stationary phase in UTLC [4, 8, 12, 13]. Electrospinning uses electrostatic forces to generate non-woven fibers from polymer solution. Electrospinning technique is simple, fast and inexpensive. Generated fibers from this technique have a high surface area to volume ratio and diameters of fibers are within micrometer down to nanometer range. For the collector, it can be a plate collector or a rotating collector. For plate collector and low speed rotating collector, random electrospun nanofibers are achieved. For high speed rotating collector, aligned electrospun nanofibers are generated. The use of aligned electrospun nanofibers as a stationary phase in UTLC can benefit the mechanical properties [14], separation efficiency, and decreasing of the analysis time [4].

Nowadays, polymers are applied as stationary phase in TLC because polymers consist of several available functional groups such as polyacrylonitrile (PAN) [4], poly(vinyl alcohol) (PVA) [8], polyvinylpyrrolidone (PVP) [15], cellulose acetate [12] and can be applied in a wide range of pH [16]. At the present, silica can be used only the pH range of 2-8. Therefore, it is normally problematic to separate basic compound. So polymer can be used instead of silica for stationary phase.

In this work, aligned electrospun PVA nanofibers (AE-PVA) were interested to prepare and used as stationary phase for UTLC to separate the amino acids. PVA is a hydrophilic, biocompatible, nontoxic and biodegradable polymer and consists of hydroxyl groups which are similar to silica. Therefore, it can be used as a polar stationary phase in UTLC. However, PVA is soluble in water which is limited for the application of stationary phase in UTLC. To enhance the stability in water, PVA was crosslinked by glutaraldehyde because glutaraldehyde is a high effective agent and resulting a low swelling PVA [17].

1.2 Objective of the research

The objective of this work is to prepare the AE-PVA nanofibers and used as stationary phase in UTLC for a separation of amino acids.

1.3 Scopes of the research

1.3.1 Preparation of AE-PVA nanofibers by electrospinning technique.

1.3.2 Optimizing the AE-PVA nanofibers by varying factors in electrospinning process such as collector distance and rotational speed.

1.3.3 Characterization of AE-PVA nanofibers by fourier transform infrared spectroscopy (FT-IR) and scanning electron microscopy (SEM).

1.3.4 Examining the efficiency of AE-PVA nanofibers as a stationary phase in UTLC.

1.3.5 Comparison of the separation performance of AE-PVA UTLC, electrospun PVA (E-PVA) UTLC and commercial silica TLC.

1.4 Benefits of the research

The AE-PVA nanofibers are able to be used as stationary phase in UTLC for the separation of amino acids.

CHAPTER II

THEORY AND LITERATURE REVIEWS

2.1 Electrospinning

Electrospinning is a technique which is used for generating fibers from polymer solution or polymer melt. This technique has several advantages such as high porosity, high surface area to volume ratio, small diameter of fibers within the range of nanometers to micrometers, controllable properties and functionality of nanofibers, simple apparatus and cost-effective. Electrospun nanofibers are used in many application such as scaffolds [18, 19], wound dressing [20, 21], drug delivery [22, 23], filtration [24, 25], biosensors [26], protective clothing [27], energy generation [28], immobilization enzyme [29], affinity membrane [30, 31] and stationary phase of TLC [8, 11, 12, 15].

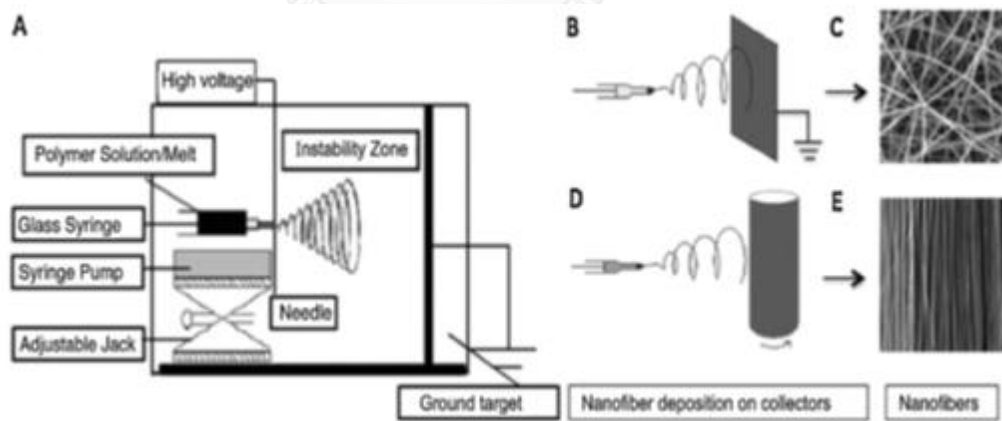


Figure 2.1 (A) schematic of electrospinning process, (B) plate collector, (C) random electrospun nanofibers collecting on plate collector, (D) rotating collector, (E) aligned electrospun nanofibers collecting on rotating collector [32].

The electrospinning setup is shown as Figure 2.1. There are three main components which are high voltage power supply, spinneret and collector. The spinneret is normally consisted of pipetted tip and syringe connected to a metal needle. For collector, there are two types of collector which are plate collector (Figure 2.1 B) and rotating collector (Figure 2.1 D).

Fibers generated from electrospinning technique are produced via the formation of Taylor cone (Figure 2.2). Without electric field, the shape of polymer solution at the tip of needle is hemispherical due to surface tension. When start applying high voltage, electric field induces charge on the surface of polymers solution. As the electric field is increased until critical point, repulsive electrostatic force is higher than surface tension which causes the polymer solution at the tip of needle elongate to form a conical shape with the initiated jet of polymer solution as known as Taylor cone. As the jet travels to collector, solvent is evaporated and non-woven nanofibers are formed on collector [32, 33]. Generally, electrospinning produces random fibers when plate collector is used. Aligned fibers are generated when the rotating collector such as rotating drum or disc drum is used at high speed rotation.

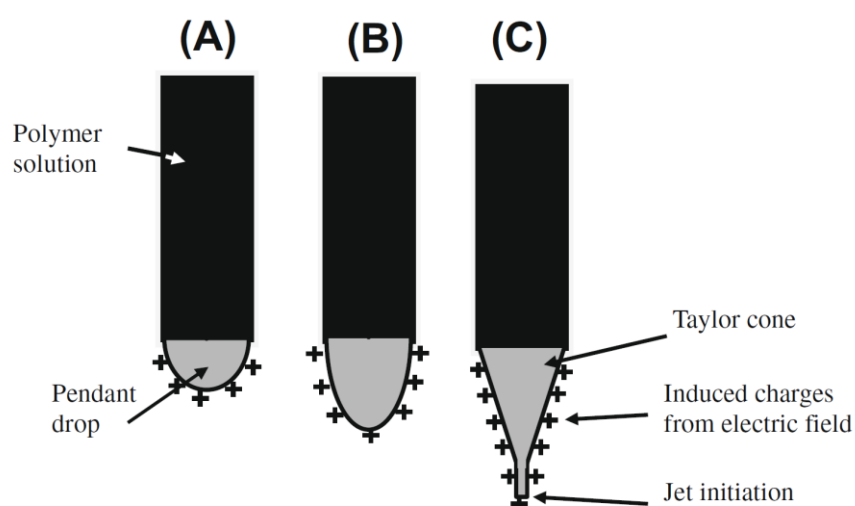


Figure 2.2 Schematic of Taylor cone formation (A) hemispherical shape, (B) elongated polymer solution, (c) Taylor cone [34].

2.2 Parameters of electrospinning technique

There are many parameters which affect the fabrication of fibers by electrospinning technique [33, 35, 36].

2.2.1 The Solution properties

2.2.1.1 Concentration

Concentration of polymer solution affects to morphology of fibers during electrospinning. As very low concentration, bead is normally observed because of low viscosity and high surface tension of polymer jet in Taylor cone. As proper concentration, smooth fibers are formed. Eda [37] showed the effect of polymer solution concentration on the morphology of polystyrene electrospun fibers as shown in Figure 2.3. SEM images of fibers formed at various polystyrene concentrations showed the generation of beads at low concentration of polymer and smooth fibers at proper concentration of polymer.

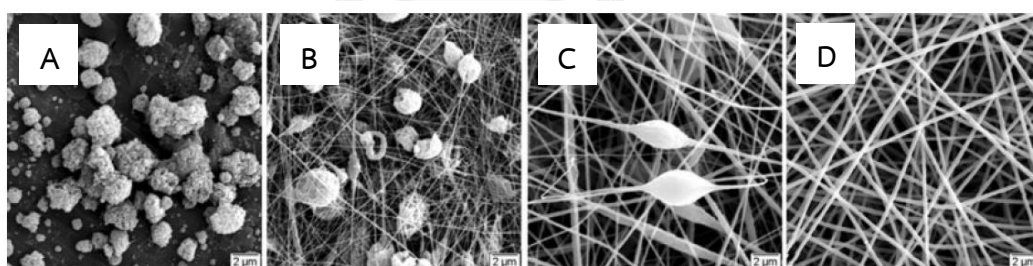


Figure 2.3 Morphology of electrospun at various concentration of polystyrene solution (A) 2.5 wt%, (B) 4.8 wt%, (C) 13.1 wt%, (D) 20.2 wt% [37].

Furthermore, increasing concentration of polymer causes the fiber diameters to increase. Yang [38] prepared polyvinylpyrrolidone electrospun nanofibers at different concentration of solutions such as 4 wt%, 6 wt% and 8 wt%.

They observed the increase of diameter of nanofibers from 20 nm to 35 nm and 50 nm, respectively.

2.2.1.2 Surface tension

Surface tension depends on polymer and solvent. Yang [38] examined this effect by prepared 4 wt% of polyvinylpyrrolidone in different solvents such as ethanol, dichloromethane and dimethylformamide. Each nanofibers are shown as Figure 2.4. Polyvinylpyrrolidone in dimethylformamide and dichloromethane (Figure 2.4 B and 2.4 C) generated bead on nanofibers because of high surface tension and low viscosity of solution. In the other hand, polyvinylpyrrolidone in ethanol generated smooth nanofibers because of proper surface tension and viscosity.

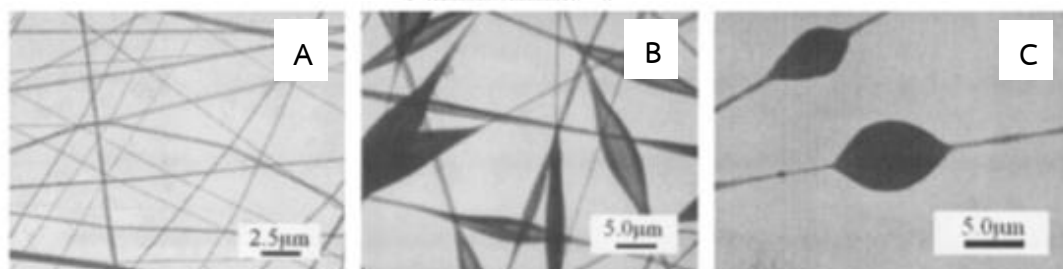


Figure 2.4 TEM of 4 wt% of polyvinylpyrrolidone dissolved in (A) ethanol, (B) dichloromethane, (C) dimethylformamide [38].

2.2.1.3 Molecular weight

Molecular weight of polymer affects to viscosity and surface tension of polymer solution. High molecular weight polymer caused viscosity of the polymer solution to be high enough to generate fibers via electrospinning technique. As low molecular weight polymer, beads were generally formed on fibers. Moreover, fibers

generated from high molecular weight polymer solution were larger than those generated from low molecular weight polymer solution.

Koski [39] studied effect of molecular weight of polymer to fiber morphology. The concentration was fixed at 25 wt% of PVA solution. SEM images of generated fibers were shown in Figure 2.5. By varying the molecular weight of PVA, smooth and fine nanofibers were generated at proper molecular weight which was 13,000-23,000 g/mol. As low molecular weight of PVA was used, beads were formed on fibers as shown in figure 2.5 (A). Moreover, too high molecular weight of PVA was resulting to flat fibers as shown in Figure 2.5 (C).

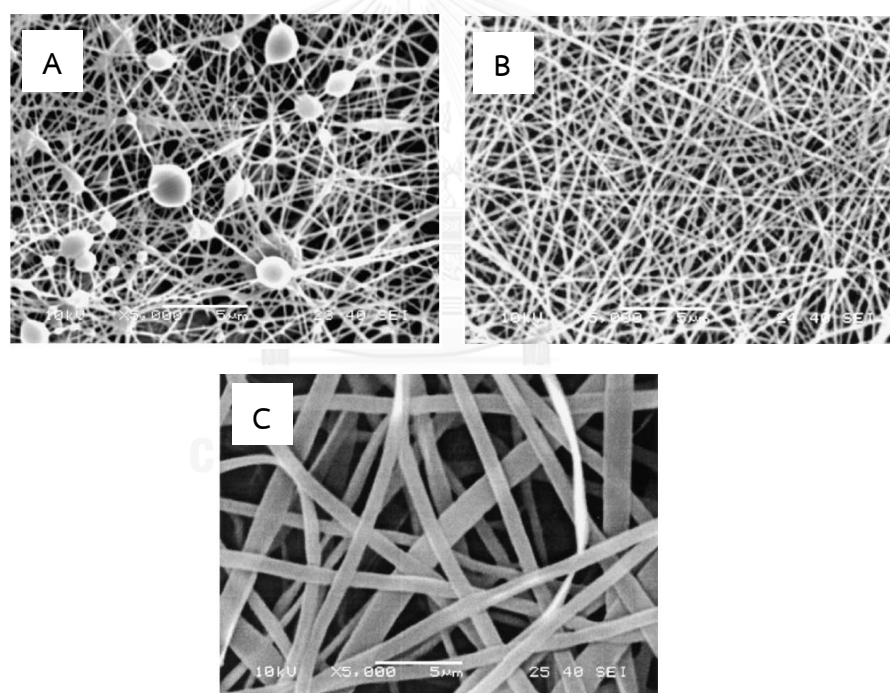


Figure 2.5 SEM images of 25 wt% PVA solution which various molecular weight (A) 9,000-10,000 g/mol, (B) 13,000-23,000 g/mol and (C) 31,000-50,000 g/mol [39].

2.2.2 Processing conditions of electrospinning

2.2.2.1 Applied voltage

Nanofibers is generated from the induced charge on the surface of polymers solution in electric field. Yuan [40] studied relation between applied voltage and morphology of nanofibers. High voltage was applied at 10 kV, 15 kV and 20 kV which diameters of generated fibers were 344 ± 55 nm, 331 ± 26 nm and 323 ± 22 nm, respectively. As increasing electrical field, diameter of nanofibers is decreased slightly as shown in Figure 2.6 because higher voltage caused an increasing of electrostatic repulsive force on the jet and also increased an evaporation rate. Therefore, diameter of nanofibers is decreased.

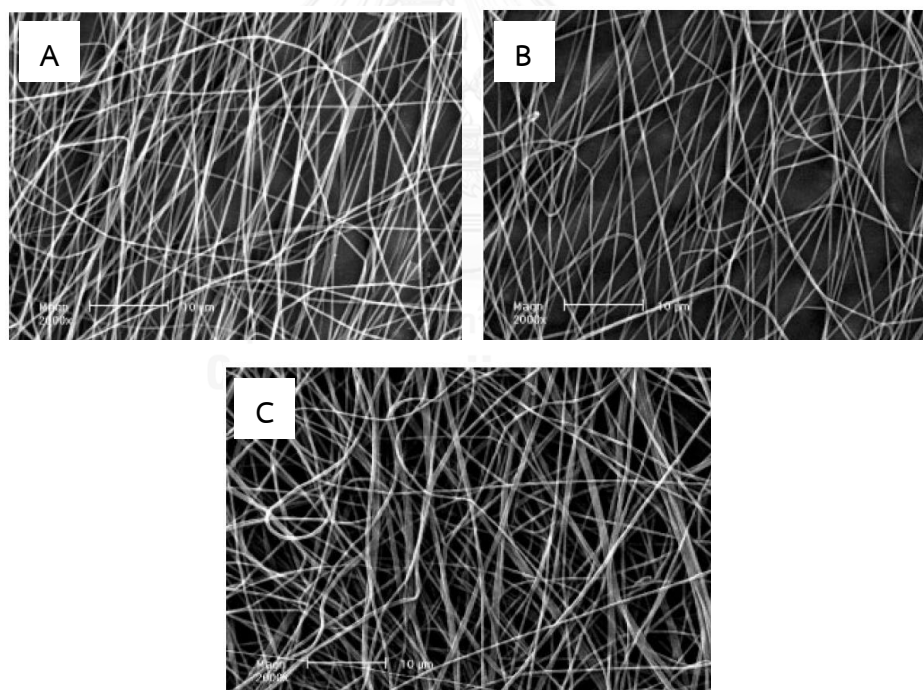


Figure 2.6 SEM images of the electrospun fibers from a 20 % polysulfone solution in N,N-dimethylacetamide/acetone. High voltage was applied at (a) 10 kV, (b) 15 kV and (c) 20 kV [40].

2.2.2.2 Distance between the tip of needle and collector or collector distance

Suitable distance makes solvent to take enough time for evaporation before polymer solution travels to collector. Supaphol [41] studied effect of distance on nanofibers morphology. 10% w/v of PVA solution was electrospun at 5 cm, 10 cm, 15 cm and 20 cm of collector distance. SEM images were shown in Figure 2.7. A short collector distance as 5 cm in Figure 2.7 (A) was produced fibers with beads on the fibers because of insufficient time for solvent evaporation. Extending collector distance to 10, 15 and 20 cm, bead on fibers were reduced as well as the diameter of fibers which were resulting from the enough time of stretching of the jet and solvent evaporation.

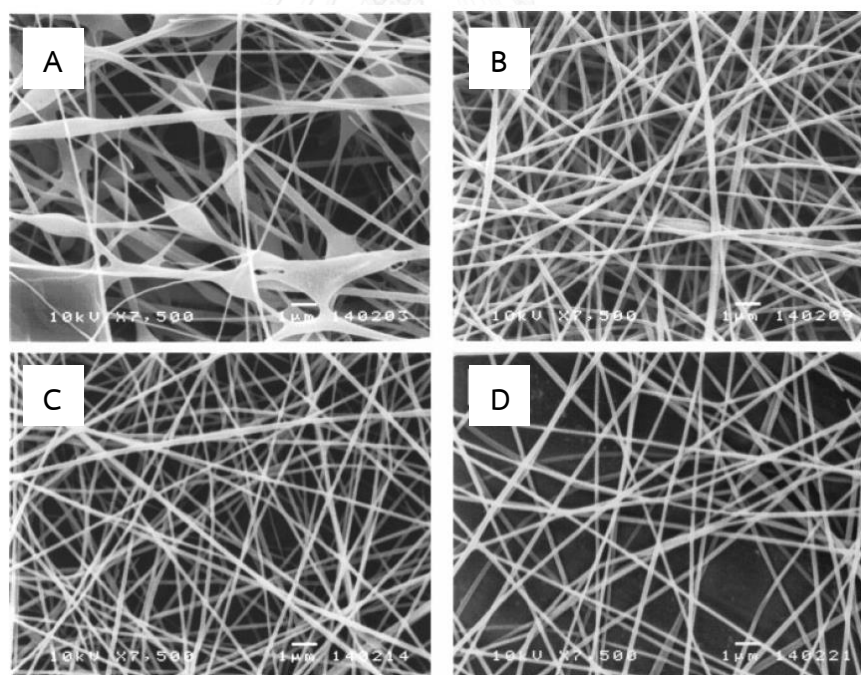


Figure 2.7 SEM images of PVA 10% w/v of PVA solution which collector distance was (A) 5 cm, (B) 10 cm, (C) 15 cm, (D) 20 cm [41].

2.2.2.3 Flow rate

Flow rate is related to the evaporation of solvent. At low feed rate, solvent got enough time to evaporate and resulting to the fine and smooth fibers. In the other hand, beads were formed on fibers when high flow rate of polymer solution was applied [36].

2.2.2.4 Type of collector

Collectors are normally a conductive substrate to support charged fibers. Aluminium foils are the simplest collectors which can be applied in various applications.

2.2.2.4.1 Plate collector

Plate collector is a stationary metal plate or foil placed at a fixed distance from a spinneret. Fibers generated on this collector are random electrospun fibers.

Lu [8] prepared electrospun PVA nanofibers which were used as stationary phase for UTLC. Collector was a plate. Nanofibers were random as shown in Figure 2.8

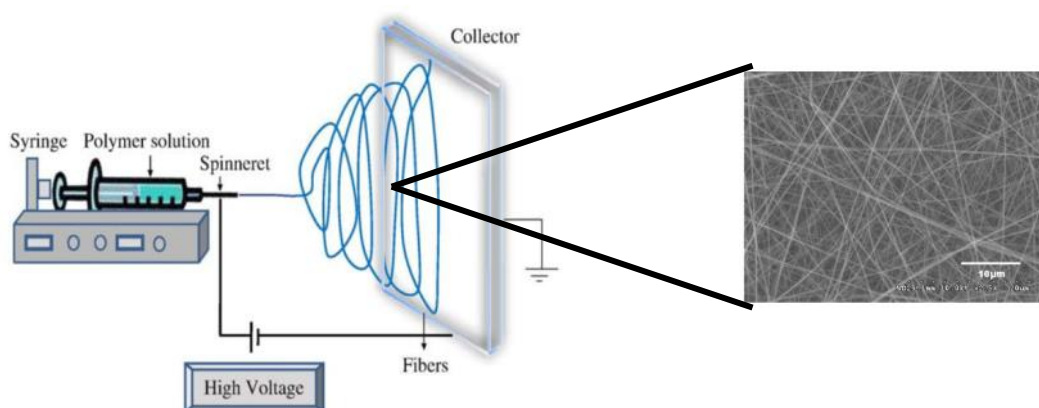


Figure 2.8 Plate collector and electrospun nanofibers [36]

2.2.2.4.2 Rotating drum

Rotating drum is a moving collector that allows an even deposition of fibers on the collector and sometimes leads to some degree of alignment of fibers. Noticeably, random electrospun nanofibers were generated at low rotational speed (Figure 2.9 (A)) and aligned electrospun nanofibers were generated at high rotational speed (Figure 2.9(B)).

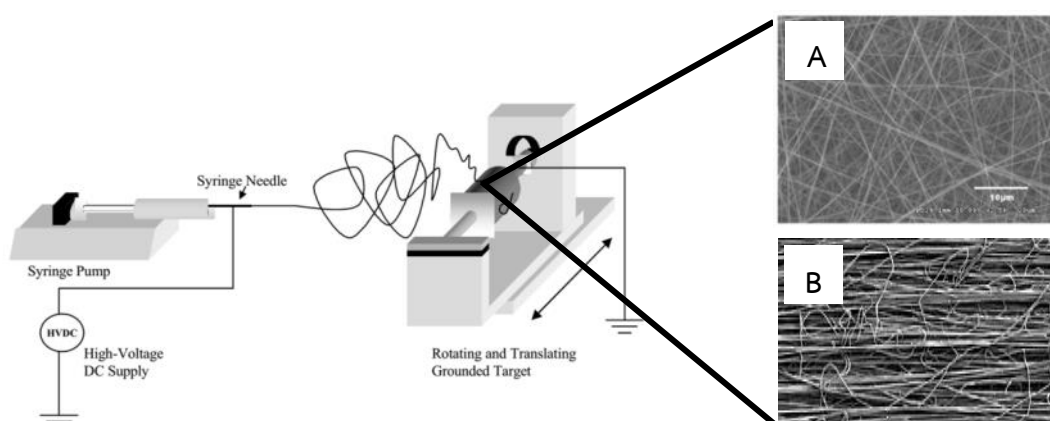


Figure 2.9 Rotating drum [42]

Supaphol [41] prepared electrospun PVA nanofibers by rotating drum at 50-65 rpm. Nanofibers were randomly deposited on the collector.

Tidjarat [12] fabricated aligned electrospun cellulose acetate nanofibers by rotating drum at 350 rpm, 4500 rpm, 6000 rpm and 7500 rpm. The results are shown in Figure 2.10. Aligned electrospun nanofibers were noticeable when rotational speed of rotating drum was above 4500 rpm.

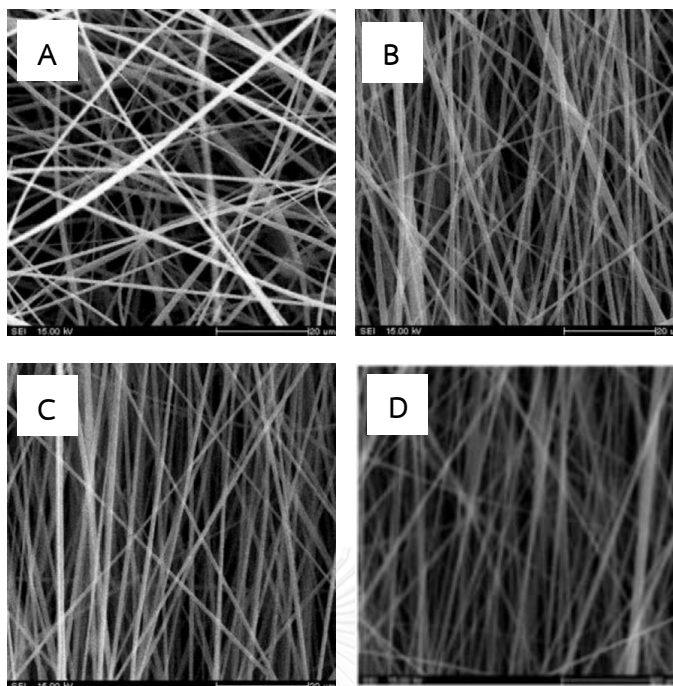


Figure 2.10 Rotational speed of (A) 350 rpm, (B) 4500 rpm, (C) 6000 rpm, (D) 7500 rpm.

2.2.2.4.3 Disc collector

Disc collector is also a moving collector. The collector geometry is shown in Figure 2.11. Disc collector also generated aligned nanofibers as same as rotating drum collector.

Beilike [4] prepared aligned electrospun PAN nanofibers by rotating disc collector at 500 rpm, 750 rpm, 1000 rpm, 1250 rpm and 1500 rpm. Disc collector is shown in figure 2.11. Aligned electrospun nanofibers was observed when rotational speed of rotating disc was more than 1000 rpm.

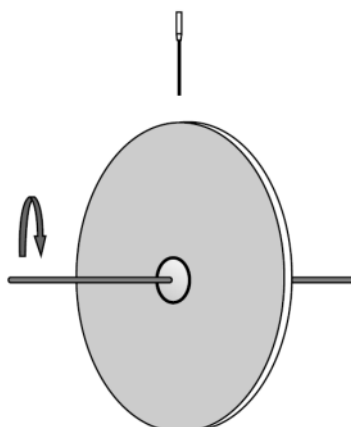


Figure 2.11 Disc collector [43].

2.2.3 Environmental conditions

Humidity in an environment during electrospinning process also affects the morphology of fibers. Increasing humidity leads to increasing number of pores on the fiber surface. As dry environment, evaporated rate of solvent is increased; however, too fast evaporation can cause the jet to be fallen before reach collector.

Casper [44] reported the effect of humidity to generated fibers during electrospinning. 35 wt% of polystyrene in tetrahydrofuran was prepared. Electrospinning was done in different humidity such as below 25%, 31-38%, 40-45%, 50-59% and 60-72% RH. As humidity was below 25%, fibers were smooth. Circular pores were found on fibers when humidity during electrospinning was above 31% RH. Amount of humidity is proportional to the number of pores on fibers as shown in Figure 2.8.

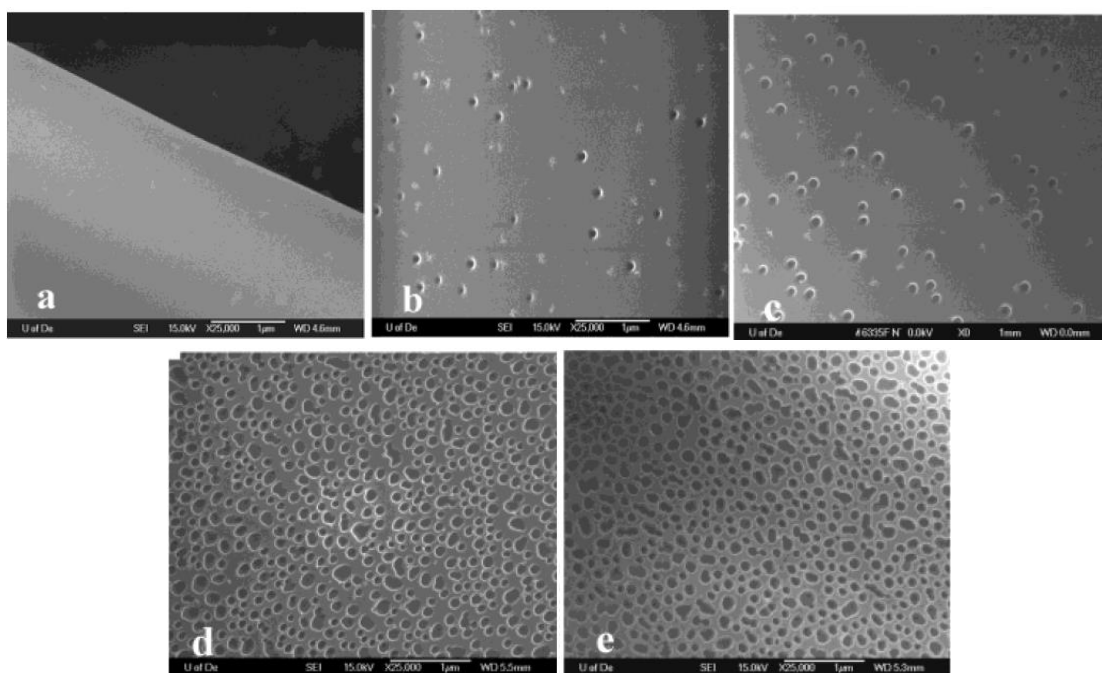


Figure 2.12 polystyrene electrospun nanofibers under different humidity (a) <math><25\%</math>, (b) 31-38%, (c) 40-45%, (d) 50-59%, (e) 60-72% RH [44].

2.3 Poly(vinyl alcohol) or PVA

PVA is a synthetic polymer which was produced by hydrolysis of polyvinyl acetate to eliminate the acetate group [45]. PVA is a semicrystalline, hydrophilic, biocompatibility, nontoxic, biodegradable, good chemical resistance, good thermal stability, good physical properties and inexpensive substance. It can be applied in various field such as industrial, commercial, medical, pharmaceutical and food. PVA is high soluble in water; however, it is insoluble in aliphatic hydrocarbons, aromatic hydrocarbons, esters, ketones, and oils [46].

Because PVA is soluble in water, it is limited to apply in the system containing water. Crosslinking the PVA can enhance the stability of PVA in water. There are many crosslink agents such as formaldehyde [47, 48], glyoxal [49], glutaraldehyde [8, 50, 51], maleic acid [52, 53], maleic anhydride [54, 55] and glycidyl acrylate [56]. Glutaraldehyde (GA) is the most used for crosslinking agents because of its effectiveness [17].

In the past, crosslinking electrospun PVA with GA consists of 2 steps [57, 58]. Firstly, electrospun PVA fibers were prepared by eletrospinning. Then electrospun PVA fibers were crosslinked by immersing them into GA and strong acid which were dissolved in acetone solution.

Recently crosslinked electrospun PVA was developed into only one step [8, 51]. PVA was in situ crosslinked while elecrospinning by adding GA and HCl into PVA solution to be crosslinking agent and catalyst, respectively.

2.4 Thin layer chromatography (TLC)

The purpose of TLC is to separate compound of mixture. Sample is spot into the stationary phase and developed in development chamber which is saturated with mobile phase. For detection of separated components, the colored compounds can be instantly visualized on the TLC plate. For colorless spot of components, spraying with detection reagent on the TLC plate should be done to make spot visible. Then the position of spot is determined by detecting in daylight or under UV light as shown in Figure 2.13. The chromatogram of sample can be characterized by position of spots comparing to the chromatograms of known reference.

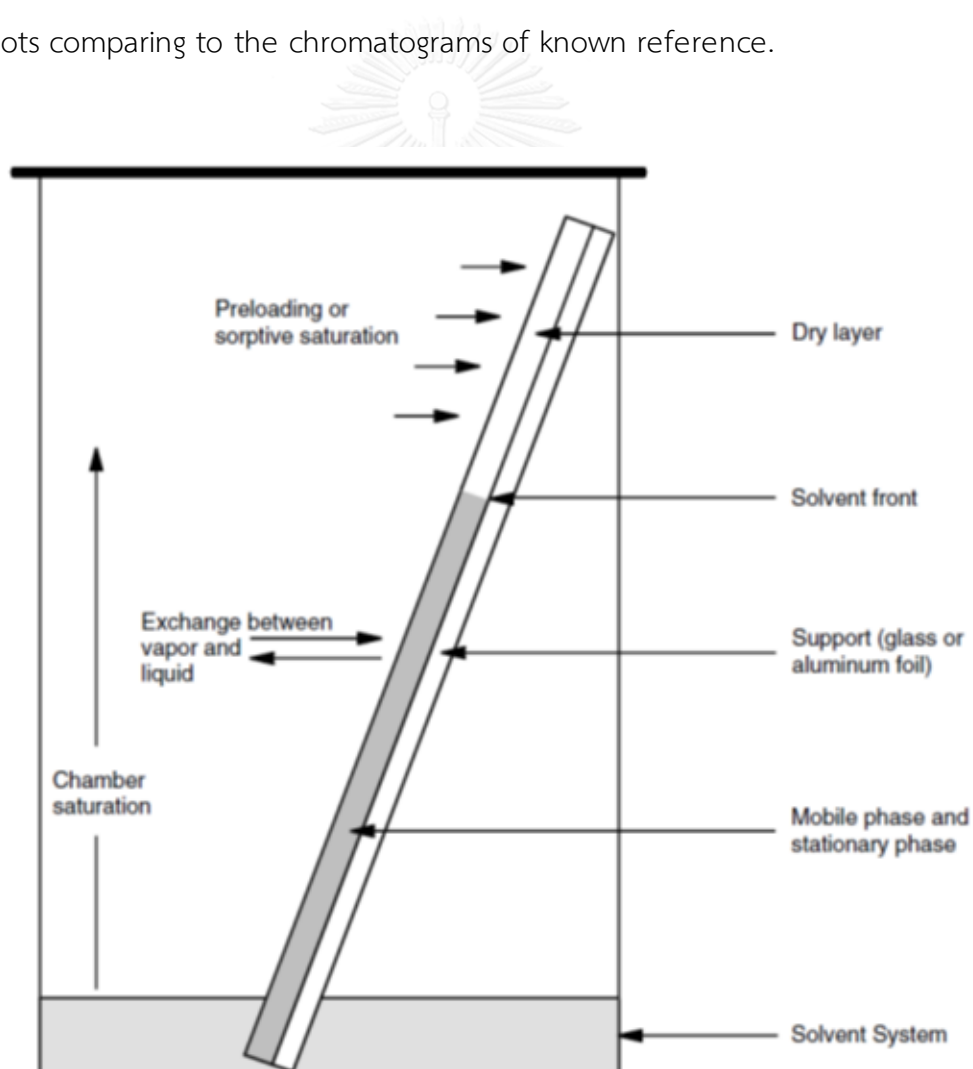


Figure 2.13 TLC plate development [59].

Separation of TLC results from interaction between molecules of stationary phase and mobile phase. Mobile phase is transported compound and migrate through stationary phase by capillary forces. Mobile phase moves upward through stationary phase. The driving force causes compound to move in direction of flow of mobile phase. The resistive forces pull compound out of the flow of mobile phase and hold compound on stationary phase by adsorption. The forces of adsorption are Van der waal's forces, dipole type interaction and complexation interactions like hydrogen bonding [5]. If compound is strongly attracted to sorbent, it will travel a short distance. In the other hand, if compound is soluble in mobile phase, it will travel a long distance.

The system of TLC consists of sample, mobile phase, stationary phase, the development chamber and detection reagent.

TLC plate consists of components as below.

1) Stationary phase

There are popular stationary phase such as

Silica consists of silanol groups (SiOH) which is naturally high acidic so the separated basic compound ability is poor and it shows broad peak tailing. The average specific surface area is 400-800 m²/g. Average pore size is 4-12 nm.

Aluminium oxide is a polar adsorbent which is similar to silica. The average particle size is between 5 and 40 µm. The specific surface area is 150-200 m²/g. Average pore size is 2-35 nm. Aluminium oxide was applied in acid form (pH 4-4.5) , neutral form (pH 7-8) and basic form (pH 9-10) [60]. Aluminium oxide can separates aliphatic compound, aromatic compound, alkaloids, steroids, terpenes and basic compound.

Cellulose is fibers which length are 2-20 µm. Cellulose consists of -OH group which can be used as polar stationary phase. Cellulose doesn't add binder

because of good self-adhesive on support. It can separate amino acids and carboxylic acids.

2) Support

Stationary phase was coated on support. Supports of TLC are made by inert material such as glass plate, plastic sheets, aluminium foil, terephthalate film and glass fiber.

3) Binder

Binder such as gypsum was filled into stationary phase to attach with support.

4) Additives

Additives such as manganese-activated zinc silicate and zinc cadmium sulfide were added into stationary phase to detect of colorless compound under UV light.

2.5 High performance thin layer chromatography (HPTLC)

HPTLC developed from TLC achieve higher separation efficiency, shorter analysis time and lower amounts of mobile phase by reducing size of particle and thickness. Particle size of HPTLC plate is smaller than TLC. The common dimension of stationary phase in HPTLC are 4-6 μm of particle size, 100 μm of layer thickness and 3-5 cm of migration distance. The average plate height in HPTLC is 12 μm . Types of sorbent are typically similar to the one used in TLC, such as silica.

2.6 Ultrathin layer chromatography (UTLC)

UTLC is thinner than either TLC or HPTLC. The thicker layer benefits faster separation, higher sensitivity and less reagent consumption. UTLC was prepared by several materials as below.

2.6.1 Monolith

The thickness of silica monolith is 10 μm . The monolithic layer has mesopores of 3–4 nm and macropores of 1–2 μm . The specific pore volume is 0.3 mL/g. The specific surface area is 350 m^2/g . A binder in the layer is not needed. Monolithic silica can separate amino acids and pesticides [3].

Barkry [6] prepared poly (butyl methacrylate-co-ethylene dimethacrylate) monolith by photoinitiated polymerization. Thickness is 50-200 μm . It can separate peptide and protein. Developed time is 5-6 min. Migration distance 6 cm.

2.6.2 Nanostructure

Nanostructure can be fabricated using glancing angle deposition (GLAD). Jim [10] prepared nanostructured thin film of silica (Figure 2.14) and used as stationary phase in UTLC. The thickness of stationary phase layer was 4.6-5.3 μm . It was used to separate dye mixture. Developed time was less than 2 min with the migration distance of 10 mm. For separation behavior, this UTLC has a plate number of 150-540 and a plate height of 12-28 μm .

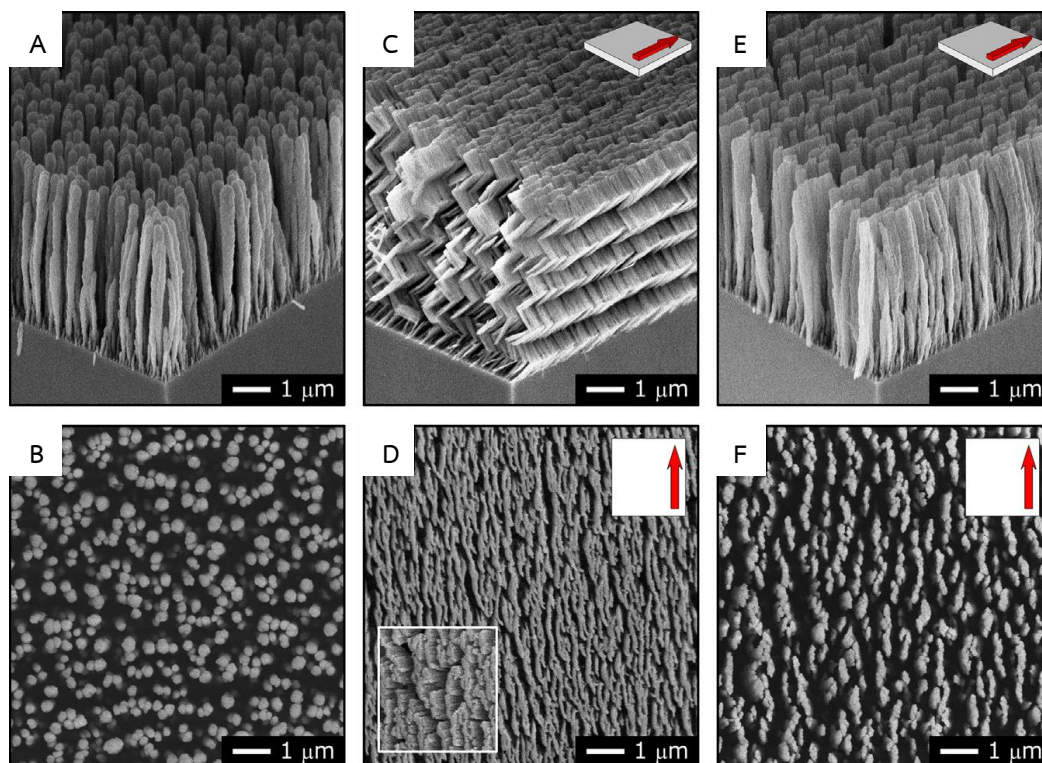


Figure 2.14 SEM image of macroporous GLAD thin film (A and B) isotropic, (C and D) anisotropic and (E and F) blade-like [10].

2.6.3 Electrospun nanofibers

Electrospinning is a simple technique for fiber fabrication. The thickness and diameter of fibers can be adjusted by flow rate, high voltage power supply, collector distance, electrospinning time and polymer type.

Lu [8] prepared electrospun PVA nanofibers by electrospinning technique. Average diameter of fibers was 190 nm. Thickness of layer of UTLC stationary phase was 15 μm . It was used to separate amino acid. The obtained PVA UTLC has a plate height of 30-70 μm .

Clark [11] prepared electrospun PAN nanofibers by electrospinning technique. Average diameter of fibers was 400 nm. Thickness of layer of UTLC stationary phase was 25 μm . It was used to separate steroidal. The PAN UTLC result a plate number of 5300-29000.

CHAPTER III

EXPERIMENTAL

3.1 Chemicals and materials

1) Poly(vinyl alcohol) (PVA, molecular weight 72000 g/mol, $\geq 98\%$ hydrolyzed)

(Merck, Germany)

2) Glutaraldehyde (GA, 25% in aqueous solution) (Merck, Germany)

3) Hydrochloric acid (37%) (Merck, Germany)

4) Glacial acetic acid (100%) (Merck, Germany)

5) Ammonia solution (28%) (Merck, Germany)

6) n-Butanol (PANREAC, EU)

7) Ethyl acetate (CARLO ERBA, France)

8) Methanol (Merck, Germany)

9) Ninhydrin (Australia, Asia Pacific Specialty Chemicals)

10) L-Alanine (Ala, $\geq 98\%$ TLC) (Sigma-Aldrich, USA)

11) L-Glutamine (Gln, $\geq 99\%$ TLC) (Sigma-Aldrich, Brazil)

12) L-Methionine (Met, $\geq 98\%$ TLC) (Sigma-Aldrich, Japan)

13) L-Phenylalanine (Phe, $\geq 99\%$ TLC) (Sigma-Aldrich, USA)

14) L-Threonine (Thr, $\geq 98\%$ HPLC) (Sigma-Aldrich, USA)

15) TLC silica gel 60 F₂₅₄ (particle sizes 5-40 μm) (Merck, Germany)

16) Aluminium foil (Diamond, USA)

3.2 Preparation of solution

3.2.1 Amino acid standard solutions

3 mg/mL of each amino acid standard solution was prepared by dissolving 9 mg of each amino acid in 3 mL of solvent system shown in Table 3.1

Table 3.1 Solvent for preparing amino acid standard solutions

Amino acids	Solvent
Alanine	water : methanol (1:4 by volume)
Glutamine	1M HCl : methanol (1:4 by volume)
Methionine	1M HCl : methanol (1:4 by volume)
Phenylalanine	water : methanol (1:4 by volume)
Threonine	1 M NH ₃ OH : methanol (1:4 by volume)

3.2.2 Ninhydrin solution

3 mL/mg of ninhydrin solution was prepared by dissolving 15 mg of ninhydrin in 5 mL of n-butanol and 150 μ L of acetic acid. The solution was then sonicated at room temperature for 15 min.

3.2.3 Developing solvent for TLC separation

The amino acids standard solutions were spotted on the aligned electrospun PVA (AE-PVA-UTLC) plate, electrospun PVA (E-PVA-UTLC) plate and silica-gel TLC plate. The condition was summarized in Table 3.2. All the plates were developed in 100 mL beaker, covered with a watch glass. The mobile phase was equilibrated for 10 min before each development.

The detection of amino acids on TLC plates was visualized by ninhydrin reaction. The ninhydrin solution was sprayed on TLC plates and heated at 100°C for 4 min.

Table 3.2 The condition of all TLC separation

	AE-PVA-UTLC	E-PVA-UTLC	Silica-gel TLC
Plates size (cm)	2×5	2×5	2×5
Developing distance (cm)	3.0	3.0	3.0
Developing solvent	n-butanol:glacial acetic acid:water (12:3:5 by volume)		
Analyte volume (nL)	25	25	200
Volume of developing solvent (mL)	3	3	6
Separation time (min)	2-6	12-13	13-14

3.3 Methodology

3.3.1 Preparation of aligned electrospun PVA nanofibers

Preparation of aligned electrospun PVA nanofibers was based on the method of Lu and Olesik [8]. The PVA aqueous solution, 10% (w/w), was prepared by dissolving 2 g of PVA powder in 18 mL of water at 80 °C and continuous stirring for 3 h until the PVA solution was homogeneous. Then the PVA solution was cooled down to room temperature. 447 µL of glutaraldehyde solution (GA:PVA, 90:1; mol/mol) was added as crosslinking agent. The mixture of the PVA solution and glutaraldehyde solution was stirred at room temperature for 10 min. 1 mL of 0.5 M hydrochloric acid solution (HCl:GA, mol:mol, 1:5) was added as catalyst and constantly stirred for 5 h at room temperature.

The crosslinked PVA solution was then used to prepare the aligned electrospun PVA (AE-PVA) nanofibers by electrospinning technique. The electrospinning was set up as Figure 3.1. The PVA solution was filled into a 3 mL of plastic syringe with 20 gauge stainless-steel, blunted end. The flow rate of the PVA solution was controlled by Prosense B.V. syringe pump at 7 $\mu\text{L}/\text{min}$. The high voltage of 24 kV from power supply (series 230, BERTAN, Hicksville, New York, USA) was applied. A rotating collector (8.5 cm \times 23 cm) was covered with aluminum foil. Alignment of nanofibers were optimized by varying speed of rotating collector to 500 rpm, 750 rpm, 1000 rpm, 1250 rpm and 1500 rpm, and distance between the tip of needle and rotating collector to 15 cm and 20 cm. The humidity of environment was controlled below 40% of relative humidity. After that, the PVA nanofibers were divested from rotating collector and dried in desiccator at room temperature for 48 h. The AE-PVA UTLC, which thickness of 20-25 μm , was cut into 2cm \times 5cm for TLC separation.

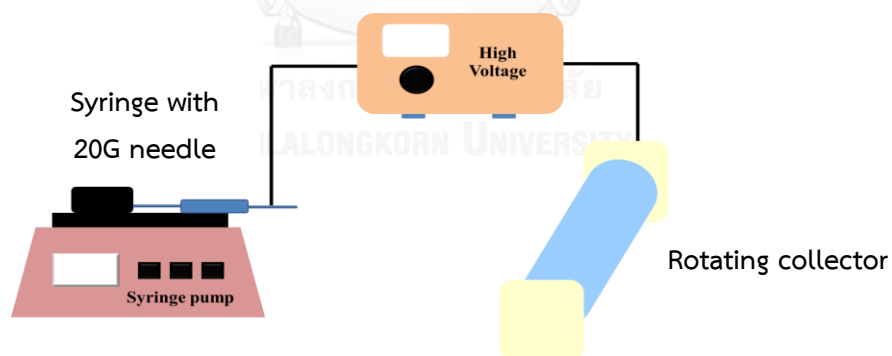


Figure 3.1 Electrospinning process setup.

3.3.2 Characterization of aligned electrospun nanofibers

3.3.2.1 Fourier Transform Infrared Spectroscopy (FT-IR)

FT-IR was used to characterize the functional groups of native PVA powder and crosslinked PVA nanofibers (AE-PVA and E-PVA). Infrared spectra (IR) were measured in attenuated total reflectance (ATR) mode using Nicolet 6700 FT-IR spectrometer. The wavenumber varied between 400 and 4000 cm^{-1} . Each sample was scanned 32 times at a resolution of 4 cm^{-1} .

3.3.2.2 Scanning Electron Microscopy (SEM)

The morphology of E-PVA and AE-PVA nanofibers were investigated by a JEOL Scanning Electron Microscopy (JSM-6480LV) at an accelerating voltage of 10 kV and 1000 \times in magnification. ImageJ software (shareware provided by RSB) was used for determining average diameters of nanofibers. The average diameter and standard deviation were calculated by sampling 20 fibers in the SEM image.

3.3.2.3 Alignment of electrospun nanofibers

The alignment of electrospun PVA nanofibers was determined by ImageJ software. The virtual line angle was calculated by median angle of 40 sampling nanofibers on the SEM image. The percentage of nanofibers was determined by number of samples which deviated angle from the virtual line was in range of below 5°, 5°-10°, 10°-15° and above 15° comparing to the number of total samples.

3.3.3 TLC separation

3.3.3.1 Velocity constant of mobile phase

Mobile phase transport through TLC plate has been determined by using the Lucas-Washburn equation (Eq. (1)) [4].

$$Z_f^2 = \frac{\gamma R t \cos \theta}{2\eta} \quad (1)$$

Where;

Z_f : the migration distance of mobile phase

γ : the surface tension

R : the effective capillary (or pore) radius

t : the corresponding time

η : the viscosity of the mobile phase

θ : the contact angle of the mobile phase with the stationary

phase

The velocity constant (\mathbf{K}) is another parameter that often used to describe mobile phase transport in TLC. \mathbf{K} was replaced in term $\gamma R / 2\eta$ in the Lucas-Washburn equation. The relationship between mobile phase migration (Z_f) and velocity constant of mobile phase (\mathbf{K}) is shown as Eq.(2)

$$Z_f^2 = \kappa t \quad (2)$$

3.3.3.2 Separation of amino acids

The retardation factor (R_f) was calculated for each compound using Eq. (3).

$$R_f = \frac{Z_s}{Z_f} \quad (3)$$

Where;

Z_s : The distance of analyte travel

Z_f : The distance of mobile phase travel

The separation efficiency of TLC was evaluated from the number of theoretical plate (N) and plate height (H) which is described by Eq. (4) and Eq. (5) respectively.

$$N = 16 \left(\frac{Z_s}{w} \right)^2 \quad (4)$$

Where;

Z_s : the distance traveled by the analyte front

w : the width of developed sample spot

$$H = \frac{L}{N} \quad (5)$$

Where;

N : the number of theoretical plate

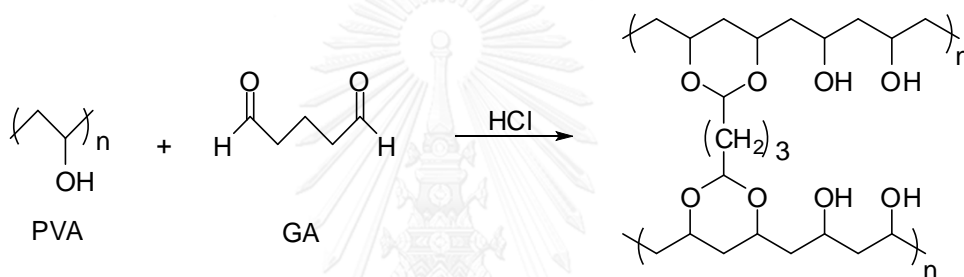
H : the plate height

L : the length of the TLC plate

CHAPTER IV

RESULTS AND DISCUSSION

Electrospun PVA (E-PVA) and aligned electrospun PVA (AE-PVA) nanofibers were prepared by electrospinning technique. Moreover, PVA was crosslinked using glutaraldehyde as a crosslinker to enhance the stability of PVA in water and polar solvent when applying as a stationary phase in TLC. The crosslinked reaction is described as Scheme 4.1.



Scheme 4.1 The reaction of crosslinked PVA.

The reaction time of crosslinking PVA was varied from 1 h to 5 h. Crosslinked PVA for 1 h-3 h result an insufficient of crosslinking as the AE-PVA plate was still swelling when immersed in the mobile phase (methanol:water, 4:1 v/v). Extend the crosslinked time to 5 h gave a better stability of AE-PVA plates in mobile phase. Therefore, PVA was crosslinked by glutaraldehyde for 5 h before fabricating the nanofibers by electrospinning technique.

4.1 Characterization of E-PVA and AE-PVA nanofibers by FTIR spectroscopy

FT-IR was used to characterize the functional groups of PVA powder and crosslinked PVA nanofibers (AE-PVA and E-PVA). The IR spectra were shown in Figure 4.1. The IR spectrum of PVA powder as shown in Figure 4.1 (a) showed the characteristic peaks of PVA at 3302, 2907, 2933 and 1015 cm^{-1} . The broad band around 3302 cm^{-1} related to O-H stretching from intermolecular and intramolecular hydrogen bonds. The two peaks of vibrational band at 2907 and 2933 cm^{-1} referred to asymmetrical and symmetrical stretching of alkyl groups, respectively. The peak of absorbance band at 1015 cm^{-1} was due to C-O-C groups. Comparing IR spectra of crosslinked PVA with PVA powder, a slightly decrease in absorbance at 3302 cm^{-1} was observed. This decrease was caused by the reaction of hydroxyl groups of PVA with dialdehyde groups of glutaraldehyde in crosslinking reaction. Moreover, the increase of absorbance around 1015 cm^{-1} , corresponding to C-O-C group was noted because acetal groups or ether groups were produced while crosslinking reaction of PVA and glutaraldehyde [61-63]. The peak intensities at 1015 cm^{-1} (-C-O-C group) and 3302 cm^{-1} (-OH group) for PVA and crosslinked PVA were ratio which were 0.20 and 0.45, respectively. IR spectra of AE-PVA nanofibers at 500 rpm, 750 rpm, 1000 rpm, 1250 rpm and 1500 rpm resulted similar peaks to E-PVA nanofibers. Therefore, both E-PVA and AE-PVA were crosslinked with GA and can be applied as a stationary phase for UTLC.

In addition, the crosslinking of PVA with glutaraldehyde in E-PVA and AE-PVA was confirmed by examining the stability of PVA nanofibers in methanol. When immersed the PVA in methanol, noncrosslinked PVA nanofibers were swelling while crosslinked PVA nanofibers could maintain the fiber morphology. This can be implied that the crosslinking reaction of PVA with glutaraldehyde was achieved.

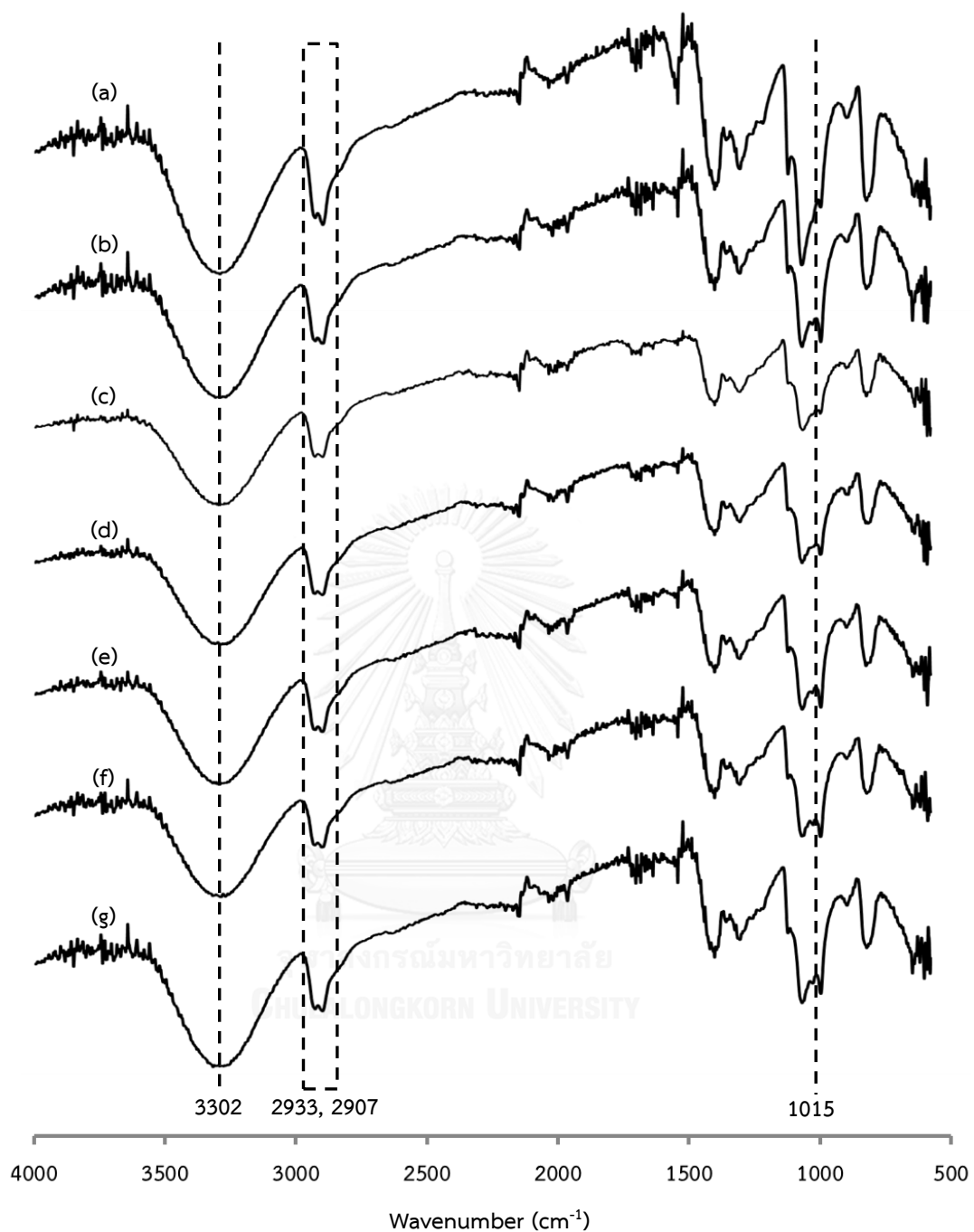


Figure 4.1 FT-IR spectra of PVA and crosslinked PVA nanofibers (a) PVA, (b) E-PVA, (c) AE-PVA at 500 rpm, (d) AE-PVA at 750 rpm, (e) AE-PVA at 1000 rpm, (f) AE-PVA at 1250 rpm and (g) AE-PVA at 1500 rpm.

4.2 Characterization of E-PVA and AE-PVA nanofibers by SEM

Morphology of E-PVA and AE-PVA nanofibers were characterized by SEM and determined the fiber diameter by analyzing SEM images using ImageJ software. From SEM images, the obtained fibers of E-PVA and AE-PVA at all studied condition were smooth without the formation of beads as shown in Figure 4.2 and 4.3. The average diameters of E-PVA and AE-PVA nanofibers were summarized in Table 4.1. It can be noted that the average diameters of E-PVA nanofibers (543±85 nm at collector distance of 15 cm and 527±88 nm at collector distance of 20 cm) were slightly larger than those of AE-PVA nanofibers which ranging from 459±71 nm to 536±80 nm at collector distance of 15 cm and from 444±55 nm to 522±62 nm at collector distance of 20 cm.

Table 4.1 Average diameter of E-PVA and AE-PVA nanofibers.

UTLC plate	Rotational speed (rpm)	Average diameter (nm) at collector distance (Mean±SD, n=20)	
		15 cm	20 cm
E-PVA	-	543±85	527±88
	500	536±80	522±62
AE-PVA	750	503±72	453±60
	1000	480±81	447±59
	1250	459±71	444±55
	1500	478±73	470±68

4.2.1 Effect of collector distance

For the same rotational speed, 20 cm of collector distance generated slightly smaller diameter of nanofibers than 15 cm of collector distance as shown in Table 4.1. This caused by the decrease of the electric field when increasing a collector distance that results to a decrease of the electrostatic repulsion force and stretching of the jet. However, the formation of beads on nanofibers was not observed from both collector distances [13] because the jet can sufficiently stretch prior to the deposition on the collector.

4.2.2 Effect of rotational speed

For both 15 cm and 20 cm of collector distances, diameters of E-PVA and AE-PVA nanofibers at slow of rotational speed (<500 rpm) were similar. Increasing the rotational speed of the collector from 500 rpm to 750 rpm produced smaller diameter of the fibers due to the stretch of the jet during the deposition on the collector. Nonetheless, the faster rotational speed than 750 rpm was not affected the diameter of electrospun PVA nanofibers but the alignment of the fibers. However, the rotational speed at 1500 rpm caused some of discontinuous of nanofibers. Therefore, the rotational speed was limited at 1500 rpm.

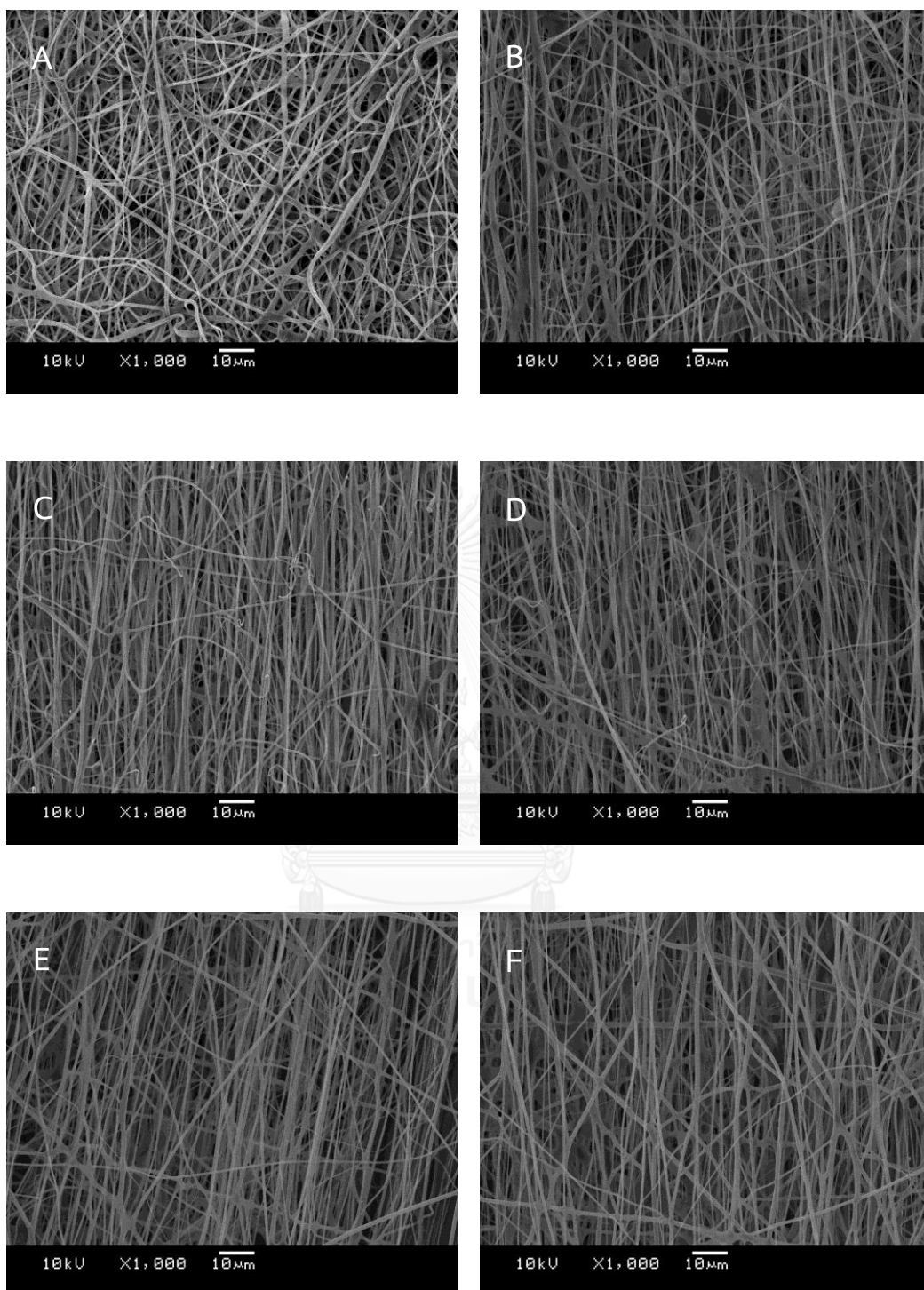


Figure 4.2 SEM images illustrating E-PVA and AE-PVA nanofibers generated on the collector distance of 15 cm. (A) E-PVA (B) AE-PVA at 500 rpm, (C) AE-PVA at 750 rpm, (D) AE-PVA at 1000 rpm, (E) AE-PVA at 1250 rpm and (F) AE-PVA at 1500 rpm.

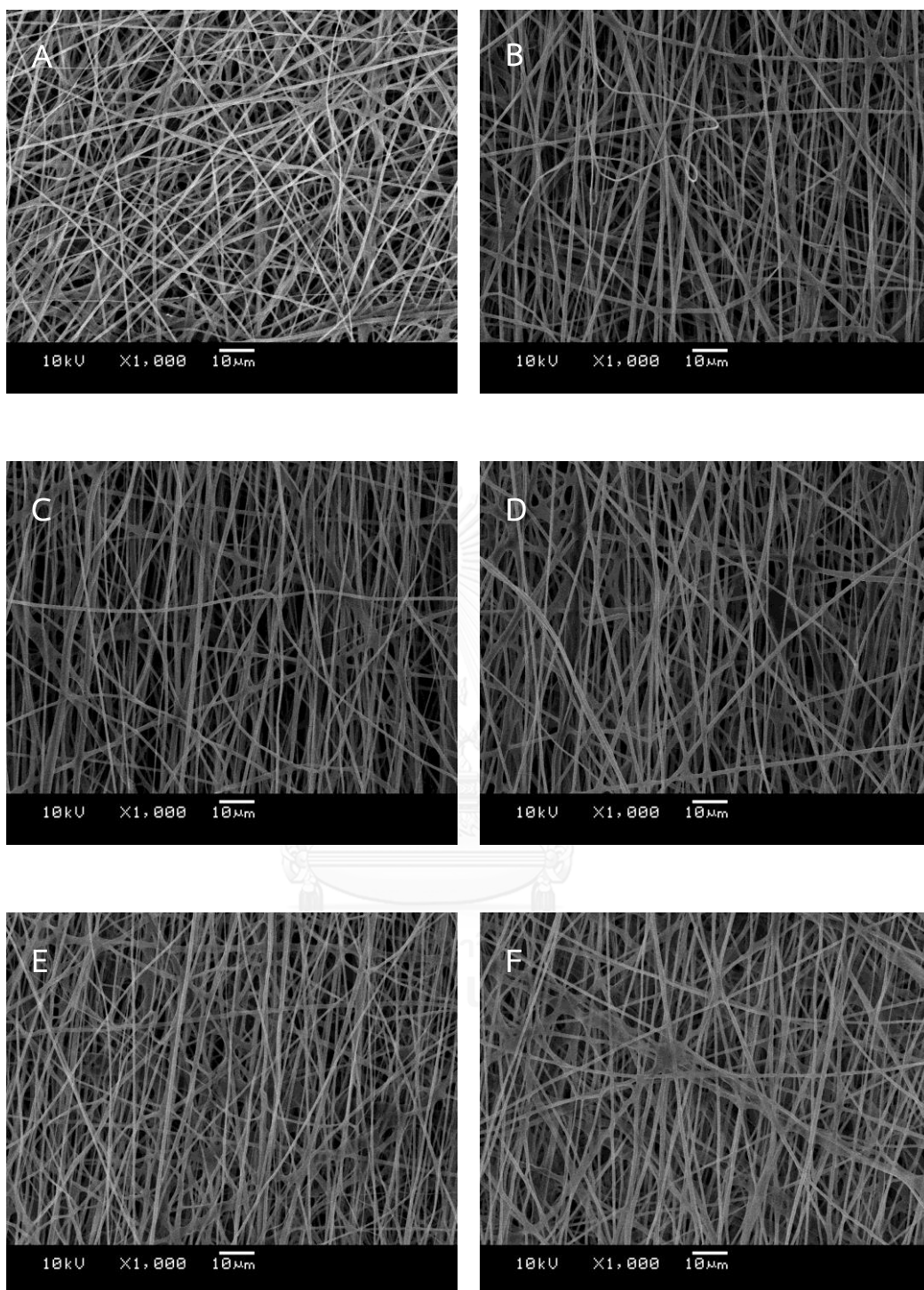


Figure 4.3 SEM images illustrating E-PVA and AE-PVA nanofibers generated on the collector distance of 20 cm. (A) E-PVA (B) AE-PVA at 500 rpm, (C) AE-PVA at 750 rpm, (D) AE-PVA at 1000 rpm, (E) AE-PVA at 1250 rpm and (F) AE-PVA at 1500 rpm.

4.3 Alignment of electrospun nanofibers

The alignment of electrospun PVA nanofibers was affected by the rotational speed of the rotating collector. The virtual lines of the alignment of the fibers were shown in Figure 4.4 for the collector distance of 15 cm and Figure 4.5 for the collector distance of 20 cm. The percentage of AE-PVA nanofibers that lined within 5° , $5-10^\circ$, $10-15^\circ$ and more than 15° angle from the virtual line were illustrated in Figure 4.6 and 4.7. The alignment of AE-PVA nanofibers generated on the collector distance of 15 cm was better than those on the collector distance of 20 cm as AE-PVA nanofibers positioned within 5° angle from the virtual line were below 50% for the collector distance of 20 cm while there were in range of 47-65% for the collector distance of 15 cm. Moreover, the alignment of AE-PVA nanofibers increased as the increase of the rotational speed. However, the alignment of AE-PVA nanofibers at 1500 rpm was decreased as the percentage of AE-PVA nanofibers positioned within 5° angle was decreased. It might be a result of discontinuous fibers. Therefore, 1250 rpm of rotational speed at 15 cm of collector distance were selected as the condition for preparing AE-PVA UTLC plate.

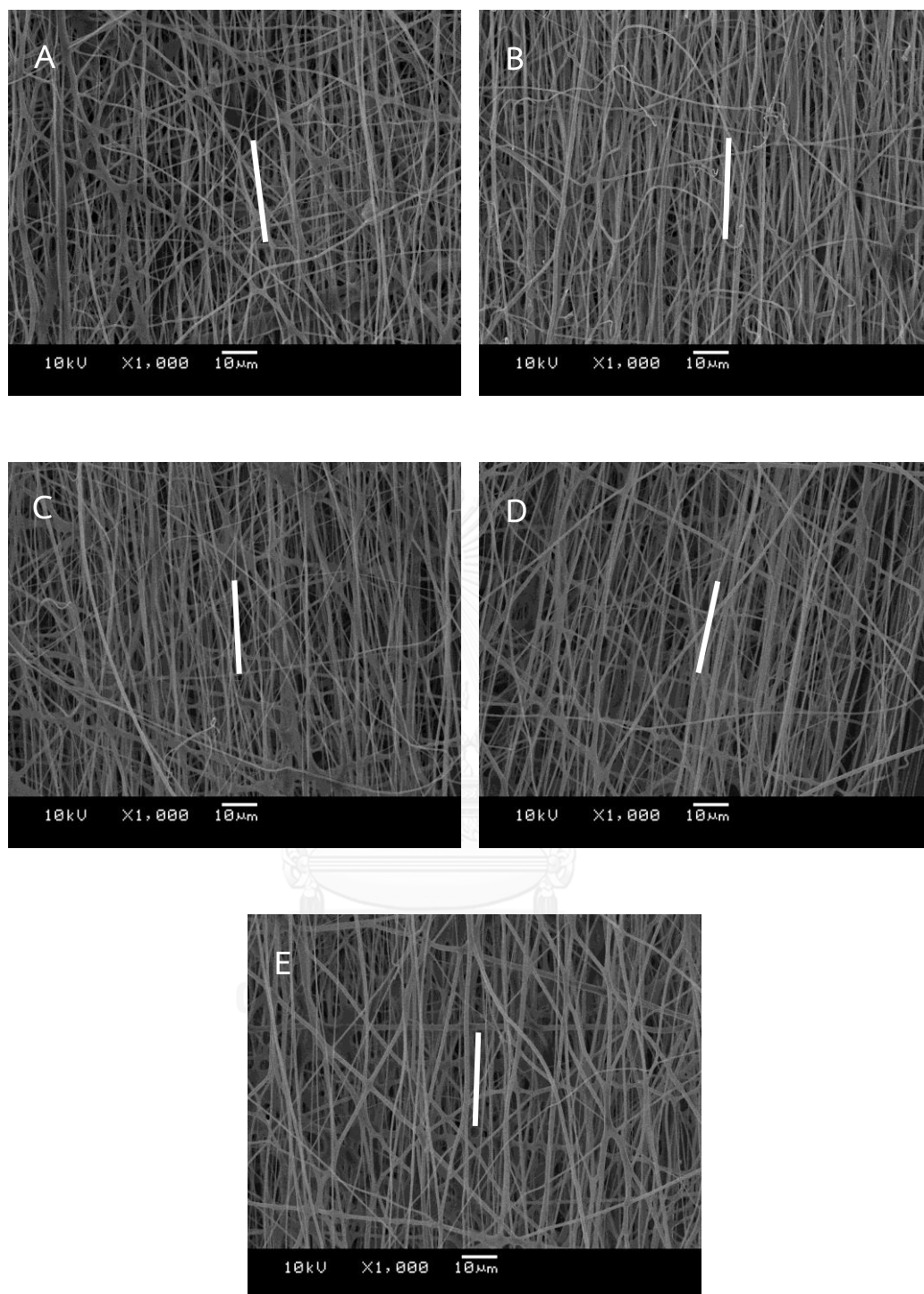


Figure 4.4 SEM images illustrating AE-PVA nanofibers generated on the rotating collector at rotational speeds of (A) 500 rpm, (B) 750 rpm, (C) 1000 rpm, (D) 1250 rpm and (E) 1500 rpm. The collector distance was 15 cm. The white line represents the virtual line of alignment of nanofibers.

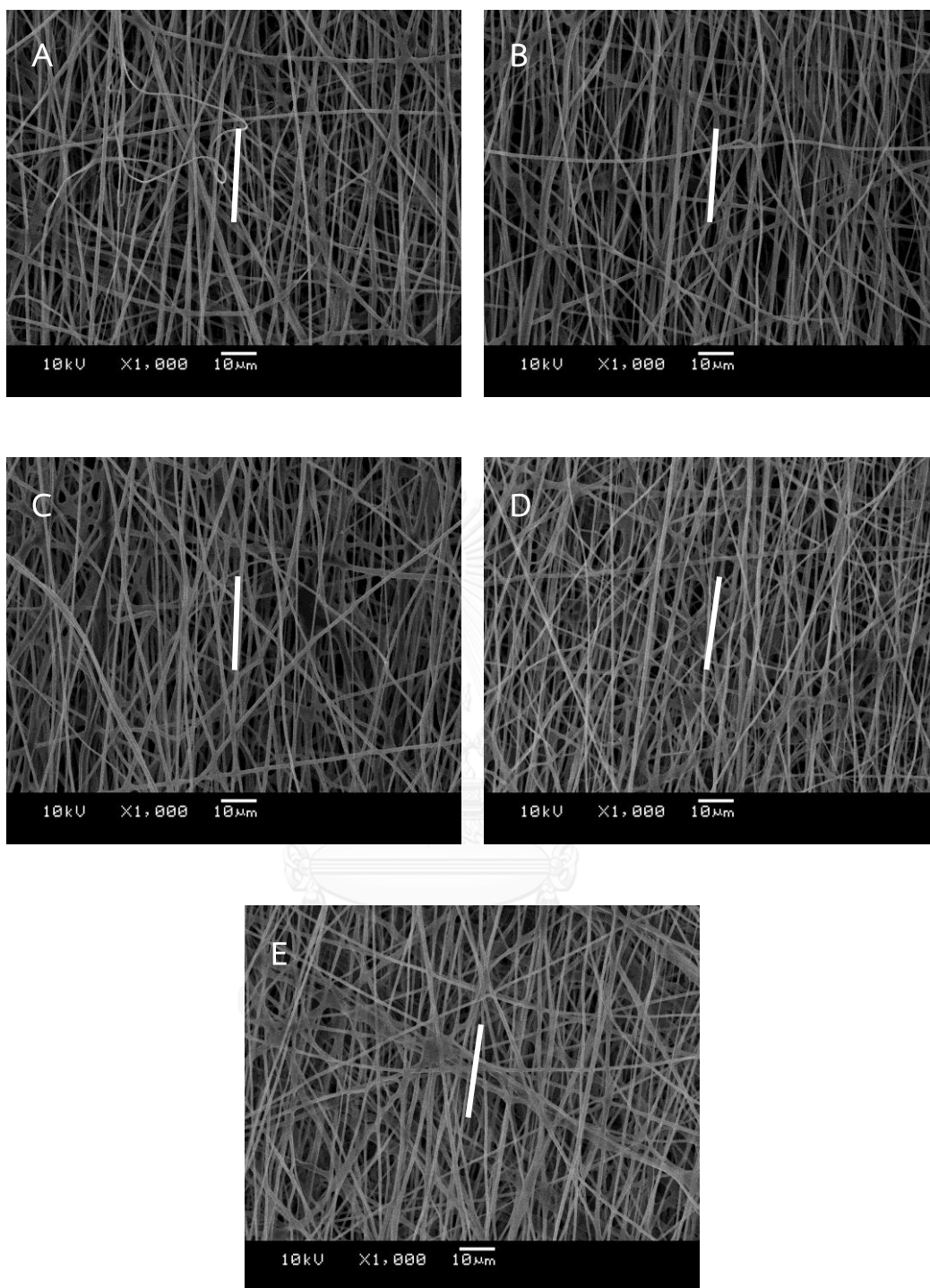


Figure 4.5 SEM images illustrating AE-PVA nanofibers generated on the rotating collector at rotational speeds of (A) 500 rpm, (B) 750 rpm, (C) 1000 rpm, (D) 1250 rpm and (E) 1500 rpm. The collector distance was 20 cm. The white line represents the virtual line of alignment of nanofibers.

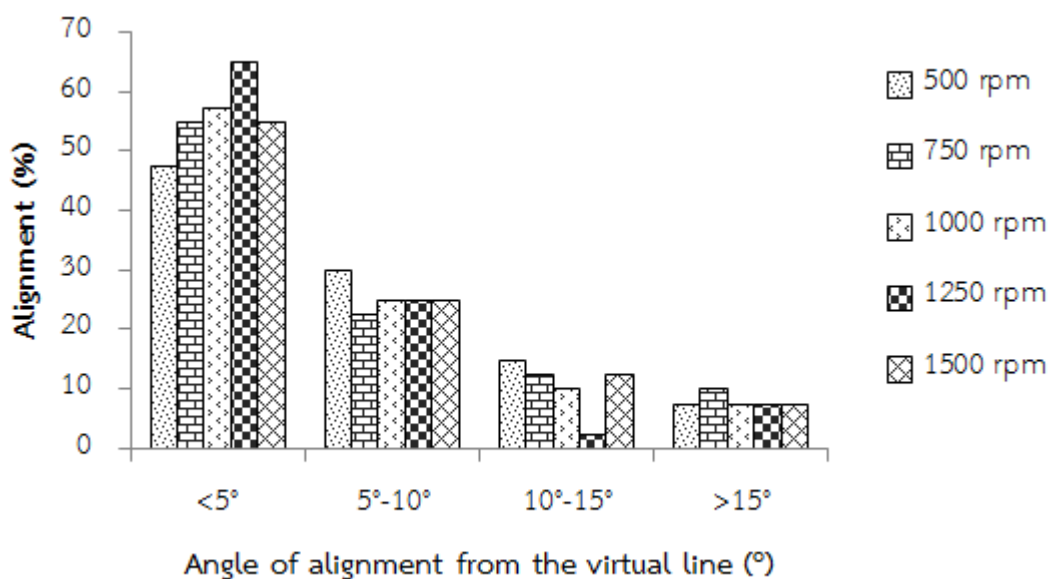


Figure 4.6 Percentage of AE-PVA fibers positioned in range of below 5°, 5° -10°, 10° - 15° and above 15° angle from the virtual line. (collector distance : 15 cm)

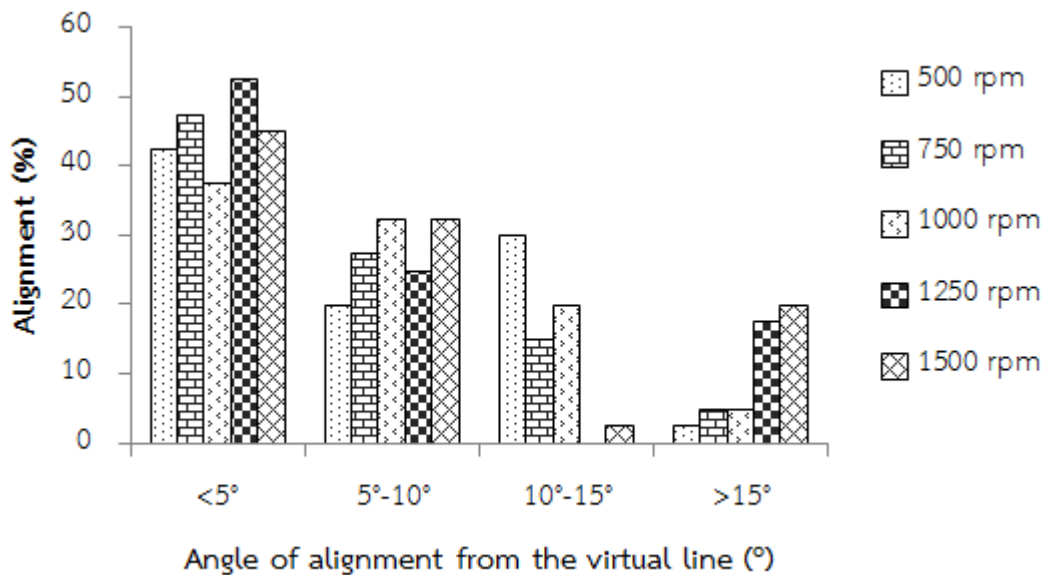


Figure 4.7 Percentage of AE-PVA fibers positioned in range of below 5°, 5° -10°, 10° - 15° and above 15° angle from the virtual line. (collector distance : 20 cm)

4.4 TLC Separation

4.4.1 Migration of mobile phase

The migration of mobile phase on AE-PVA UTLC was carried out on the mobile phase system of n-butanol : ethyl acetate : water (5:5:1 by volume). The plot between the square of migration distance of mobile phase (Z_f^2) and the time that mobile phase travelled at corresponding distance was shown in Figure 4.8. The linear relation was perceived. This indicated that the migration of mobile phase on AE-PVA UTLC plate was based on capillary flow through porous media and comparable to that in conventional silica TLC plate. Therefore, the Lucas-Washburn equation was appropriate for calculating the velocity constant of AE-PVA UTLC plate.

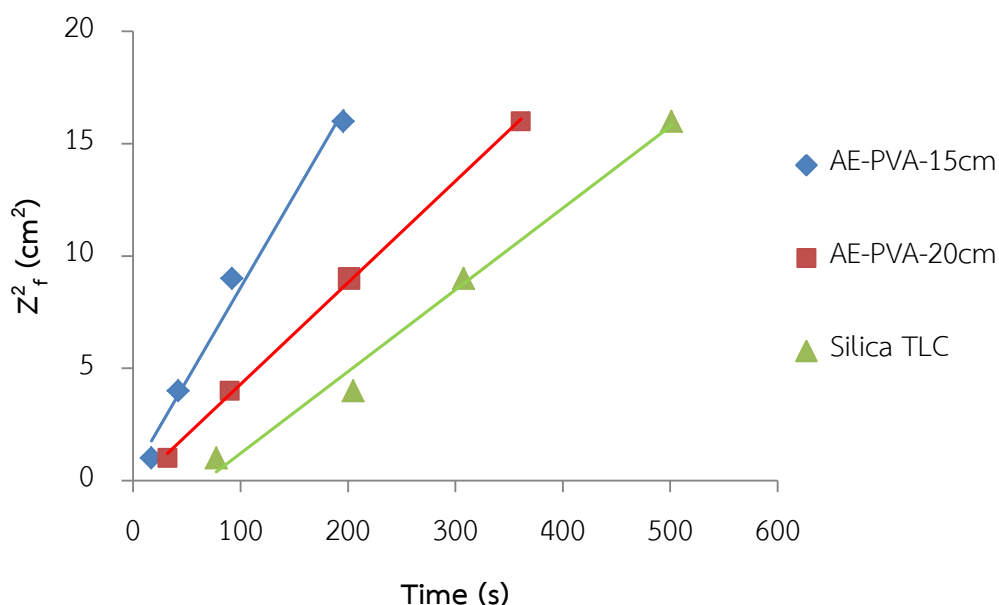


Figure 4.8 Comparison of velocity constants of mobile phase AE-PVA UTLC at rotational speed of 1250 rpm and silica TLC.

Velocity constant of mobile phase (K) of AE-PVA UTLC plate generated at various rotational speed of the collector were shown in Table 4.2 using n-butanol : ethyl acetate : water (5:5:1 by volume) as mobile phase. From Table 4.2, the velocity constant of mobile phase increased as the increase of rotational speed. This was

corresponding to the alignment of AE-PVA nanofibers on UTLC plate which enhanced the mobile phase migration via capillary force. In comparison of 15 cm and 20 cm of collector distance at optimized rotational speed (1250 rpm), K of AE-PVA-UTLC generated at 15 cm was $0.0985 \text{ cm}^2/\text{s}$ which was two times higher than that of AE-PVA-UTLC generated at 20 cm ($0.0448 \text{ cm}^2/\text{s}$) as a result of higher alignment of nanofibers on the plate generated at 15 cm. Furthermore, K of AE-PVA-UTLC was greater than that of conventional silica TLC ($0.016 \text{ cm}^2/\text{s}$) [64] and aligned electrospun silica fibers ($0.019 \text{ cm}^2/\text{s}$) [13]. As a result, the analysis time of the separation on AE-PVA UTLC can be shortened.

Table 4.2 The velocity constant (K) of AE-PVA-UTLC plates.

Z_f (cm)	Collector distance (cm)	Rotational speed (rpm)	K_{avg} (cm^2/s)	SD
3.0	15	500	0.0500	0.0003
		750	0.0600	0.0004
		1000	0.0874	0.0008
		1250	0.0985	0.0006
		1500	0.0811	0.0007
		20	500	0.0274
		750	0.0363	0.0001
		1000	0.0390	0.0001
		1250	0.0448	0.0002
		1500	0.0370	0.0001

4.4.2 Separation of amino acids

Amino acids were separated on AE-PVA-UTLC, E-PVA-UTLC and silica TLC plates to investigate chromatographic behavior. Analysis of alanine, glutamine, methionine, phenylalanine and threonine (Figure 4.9) were studied in this work. Analysis of each amino acids on AE-PVA-UTLC, E-PVA-UTLC and silica TLC were shown in Figure 4.10-4.12. R_f of each amino acids were calculated and compared in Figure 4.13.

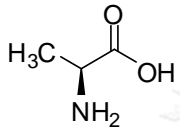
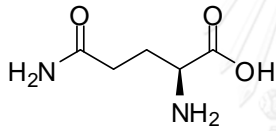
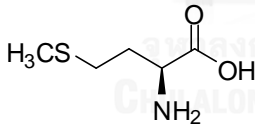
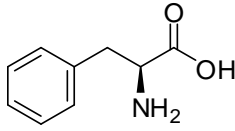
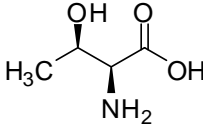
	Alanine	Ala
	Glutamine	Gln
	Methionine	Met
	Phenylalanine	Phe
	Threonine	Thr

Figure 4.9 Structure of alanine, glutamine, methionine, phenylalanine and threonine.

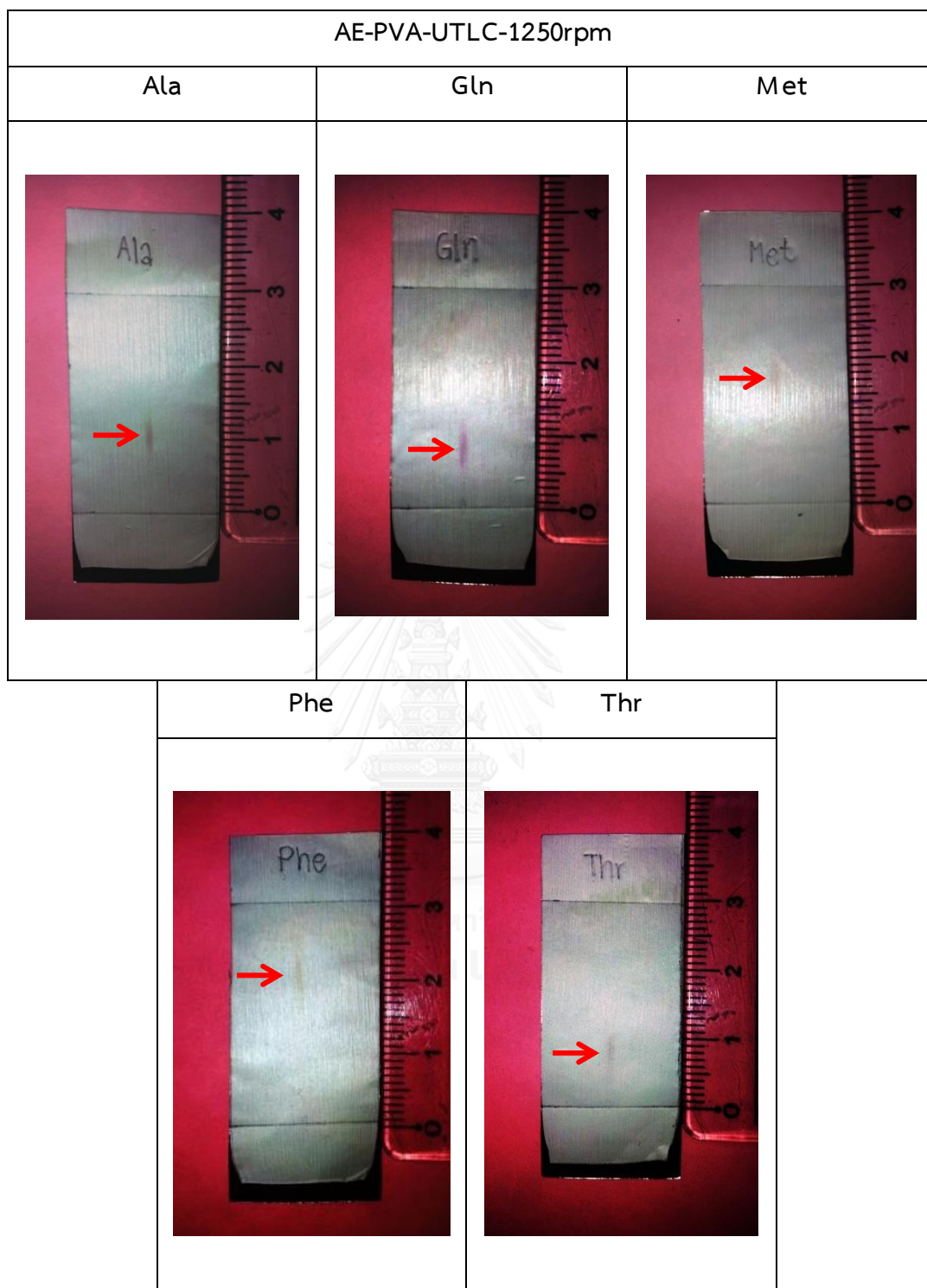


Figure 4.10 The analysis of amino acids on the AE-PVA-UTLC at 1250 rpm.

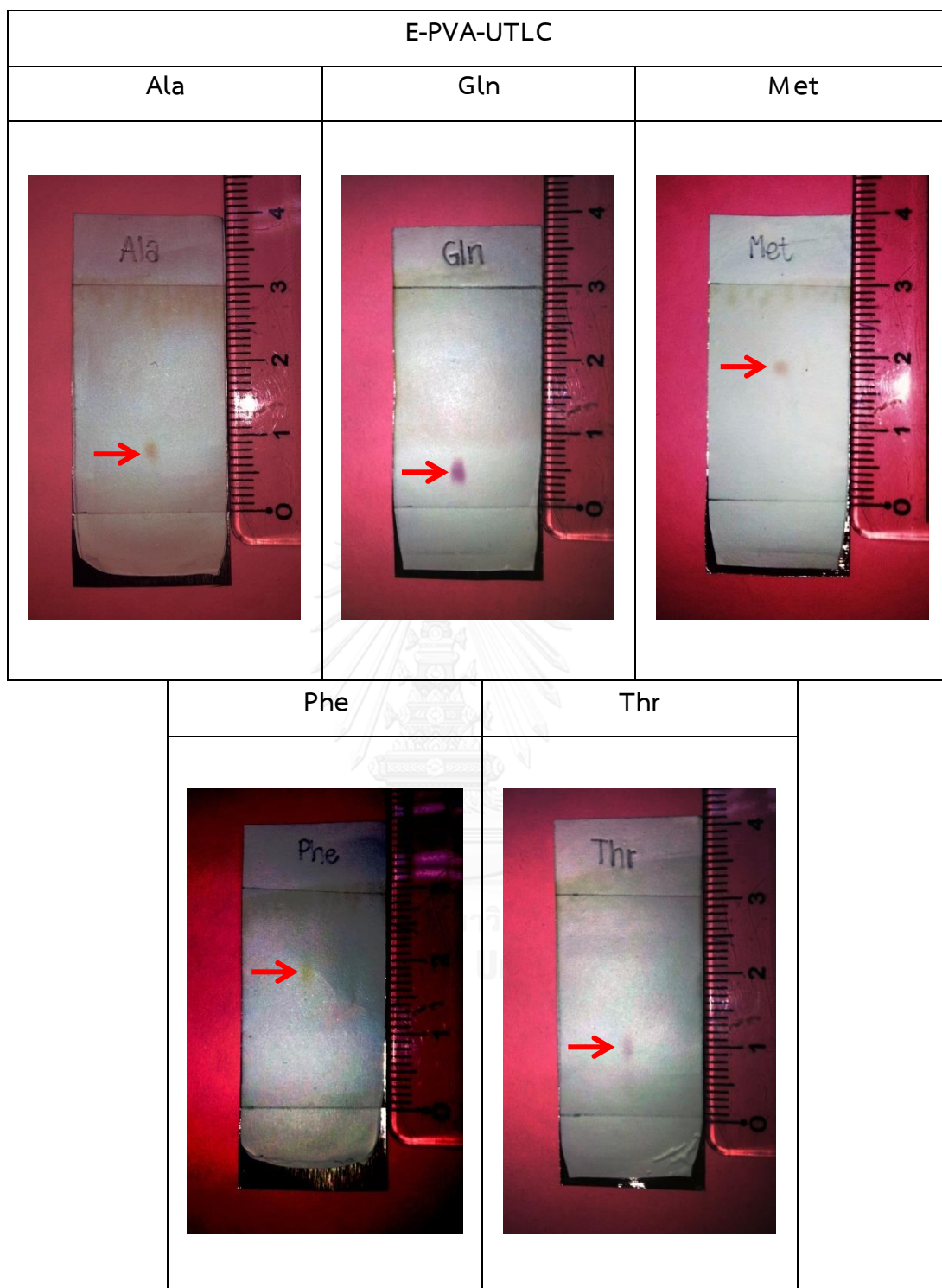


Figure 4.11 The analysis of amino acids on the E-PVA-UTLC.

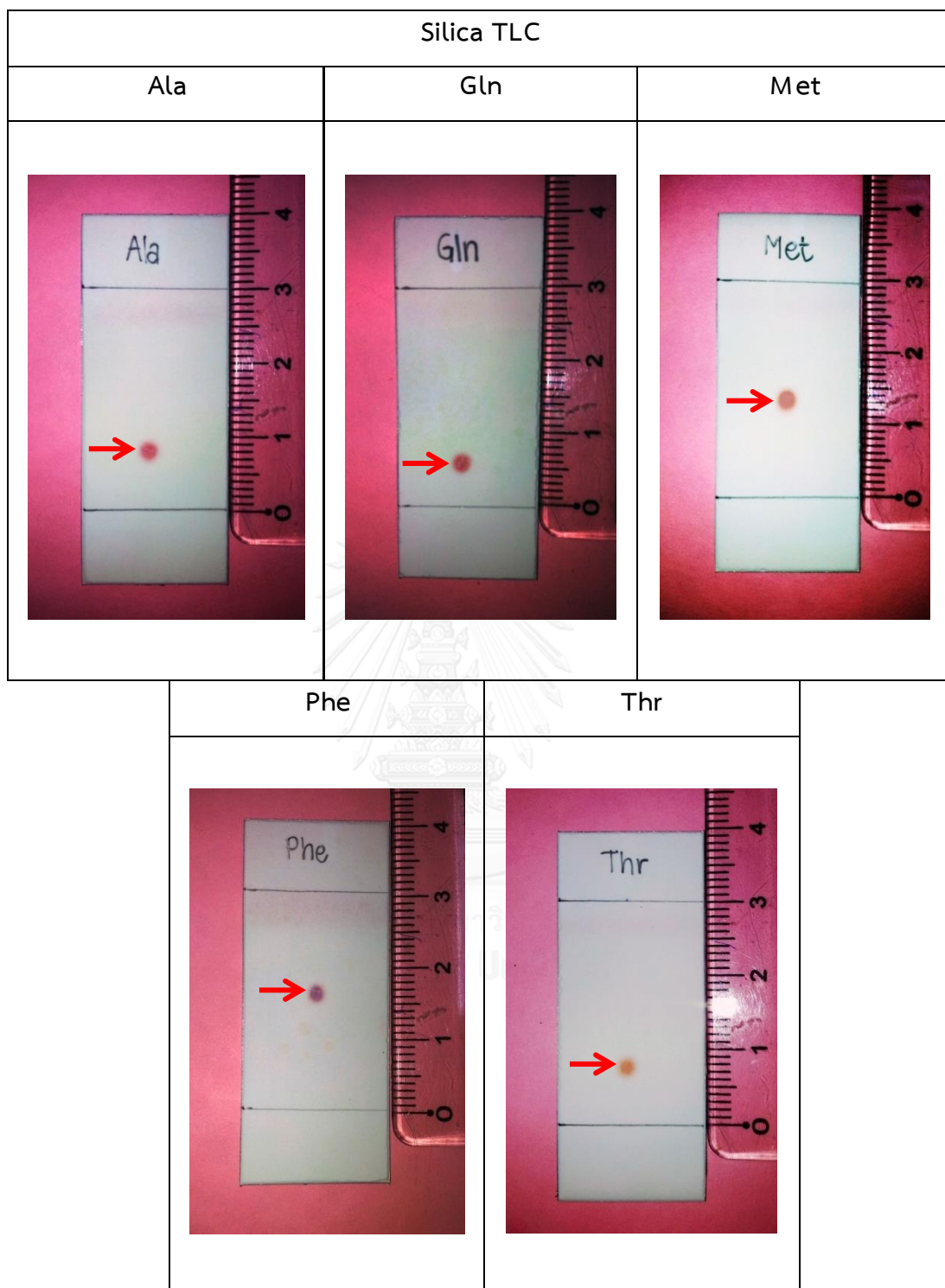


Figure 4.12 The analysis of amino acids on the silica TLC.

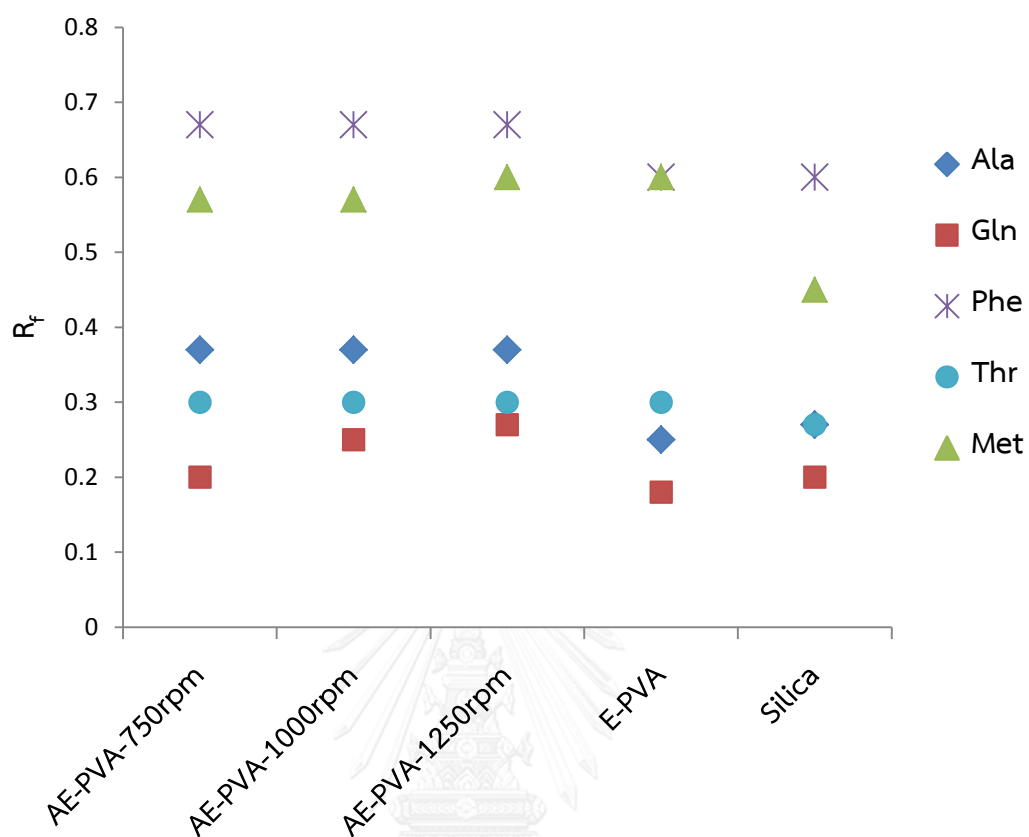


Figure 4.13 R_f of amino acids on E-PVA-UTLC, AE-PVA-UTLC and Silica TLC plate.

According to Figure 4.13, R_f of each amino acid on AE-PVA-UTLC were comparable to those analyzed on E-PVA and silica TLC plates. This indicated that AE-PVA-UTLC can apply to the TLC separation and be used as the alternative stationary phase of silica. However, slightly higher R_f on AE-PVA-UTLC was observed. This might be caused from a broad oval-shaped spot of sample when introducing the sample solution onto the AE-PVA-UTLC plate as shown in Figure 4.14.

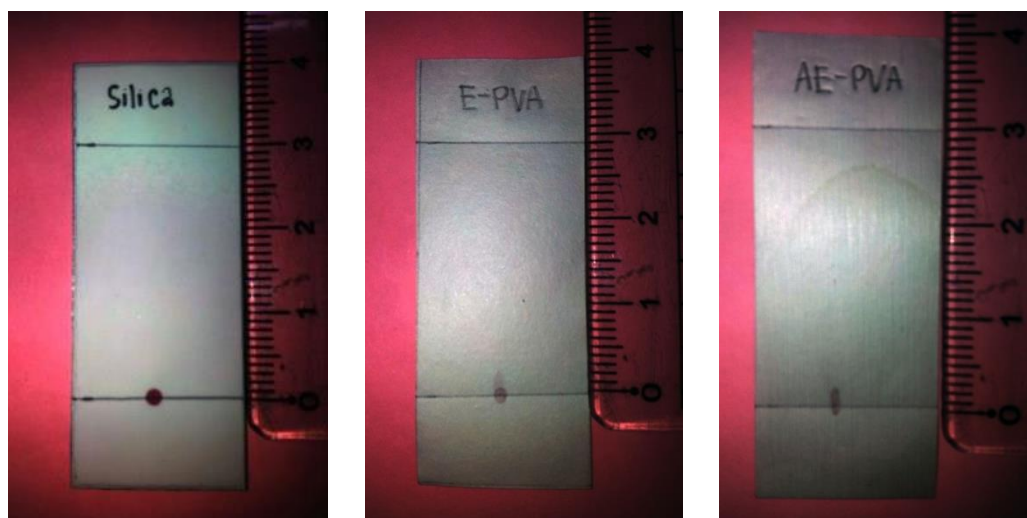


Figure 4.14 The original spot of silica TLC, E-PVA-UTLC and AE-PVA-UTLC

Separation performance of AE-PVA-UTLC was further evaluated by calculating the plate number (N) and plate height (H) as illustrated in Table 4.3. The plate numbers of AE-PVA-UTLC were 1.1-2.1 times lower than those of silica TLC and 1.2-3.3 times lower than those of E-PVA. This referred that the separation efficiency of AE-PVA-UTLC was slightly less efficient than E-PVA UTLC and silica TLC. This might be the result of width and shape of sample spot on the plate. Sample spot introducing on AE-PVA was oval with the spot size of 1.0 mm x 3.0 mm while the sample spot on E-PVA was circular with the diameter of 0.5-1.0 mm. After developing process, the spots of amino acids on AE-PVA and E-PVA were slightly broadened but at the same ration to the original spot. This can be expected that if the introduced sample spot on AE-PVA was as small as E-PVA, the separation efficiency of AE-PVA would be as good as that of E-PVA.

Nonetheless, the analysis time of AE-PVA-UTLC was greatly cut down in which 4.5 times faster than that of E-PVA-UTLC and 5 times faster than that of Silica TLC because of the higher K value of AE-PVA.

Table 4.3 Analysis time, spot width, plate number (N), plate height (H) studied of amino acids for AE-PVA-UTLC, E-PVA-UTLC and silica TLC

Amino acids	Stationary phase	Rotational speed (rpm)	Migration distance (cm)	Analysis time (min)	Spot width (cm)	N	H (μm)
Ala	AE-PVA	750	3.0	5.08	0.50	77	387
		1000		3.58	0.50	77	387
		1250		2.97	0.40	121	248
	E-PVA	-	12.50	0.15	400	75	
	Silica	-	13.70	0.20	256	117	
Gln	AE-PVA	750	3.0	5.05	0.50	23	1304
		1000		3.42	0.45	44	675
		1250		2.90	0.40	64	469
	E-PVA	-	12.30	0.25	77	387	
	Silica	-	13.75	0.25	92	326	
Met	AE-PVA	750	3.0	5.17	0.45	228	131
		1000		3.40	0.40	289	104
		1250		2.67	0.35	423	71
	E-PVA	-	12.38	0.20	900	33	
	Silica	-	13.63	0.30	324	92	

Table 4.3 (cons) Analysis time, spot width, plate number (N), plate height (H) studied of amino acids for AE-PVA-UTLC, E-PVA-UTLC and silica TLC

Amino acids	Stationary phase	Rotational speed (rpm)	Migration distance (cm)	Analysis time (min)	Spot width (cm)	N	H (μm)
Phe	AE-PVA	750	3.00	5.02	0.50	256	117
		1000		3.62	0.45	316	95
		1250		2.98	0.35	522	57
	E-PVA	-	12.50	0.25	829	36	
	Silica	-	13.67	0.25	829	36	
Thr	AE-PVA	750	3.00	4.97	0.50	52	579
		1000		3.52	0.50	52	579
		1250		2.83	0.30	144	208
	E-PVA	-	12.70	0.25	207	145	
	Silica	-	13.93	0.25	164	183	

The separation of the mixture of amino acids was also performed. The separation of the mixture of methionine and phenylalanine, the mixture of methionine and alanine, the mixture of methionine and glutamine and the mixture of alanine and glutamine were shown in Figure 4.15, 4.16, 4.17 and 4.18, respectively. Silica TLC, E-PVA-UTLC and AE-PVA-UTLC can separate most of mixture of amino acids; except the mixture of Ala and Gln because bands were overlapped. This can be implied that AE-PVA can be applied as a stationary phase in UTLC for the analysis of amino acids.

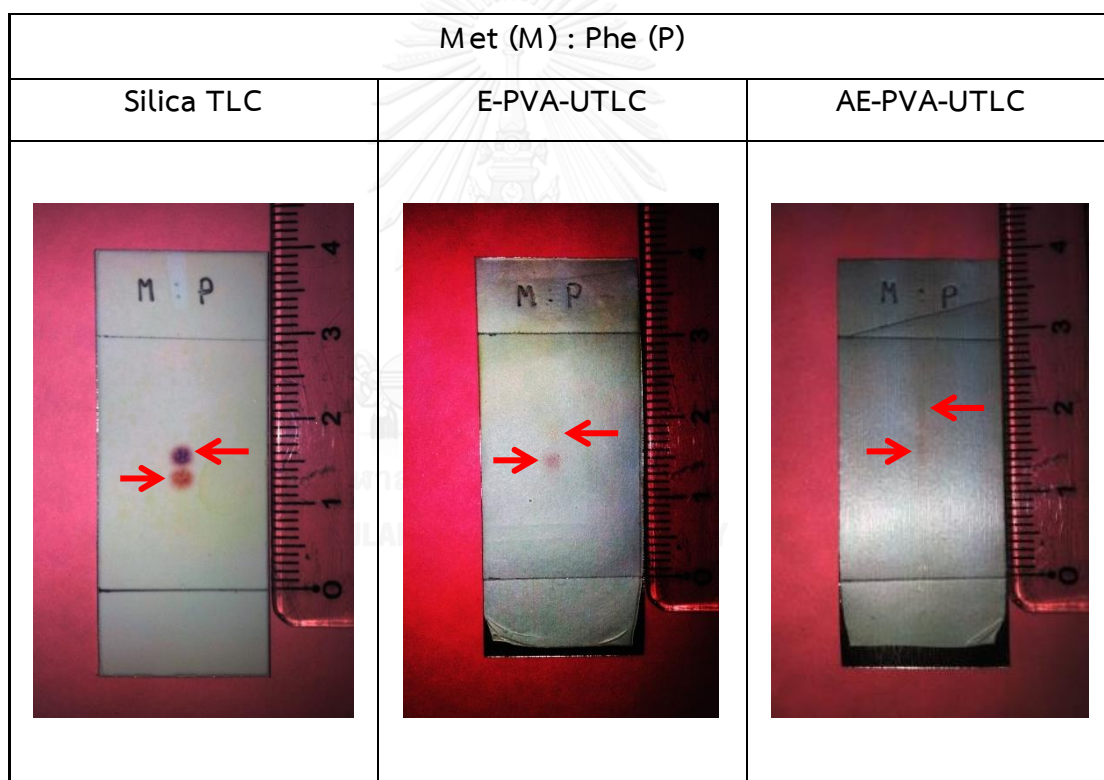


Figure 4.15 The separation of Met and Phe on the silica TLC, E-PVA-UTLC and AE-PVA-UTLC.

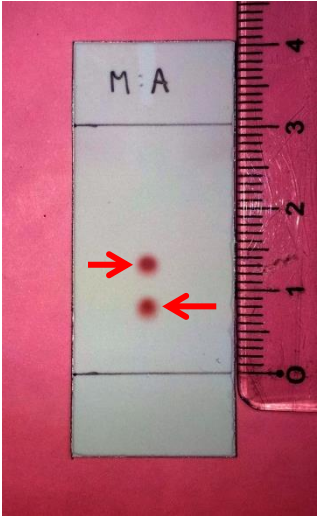
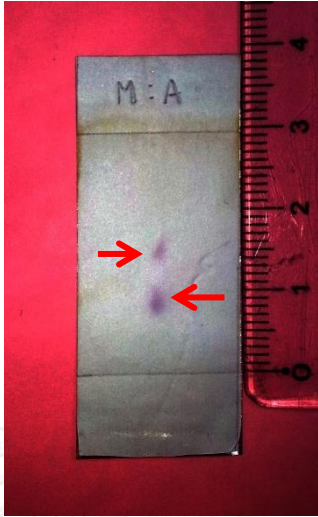
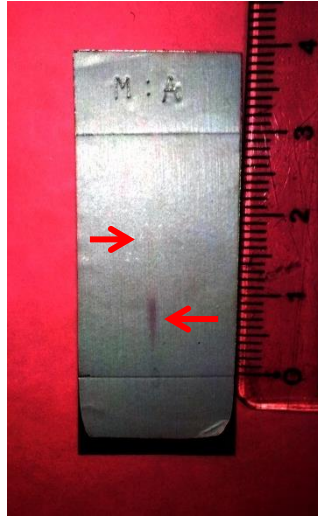
Met (M) : Ala (A)		
Silica TLC	E-PVA-UTLC	AE-PVA-UTLC
		

Figure 4.16 The separation of Met and Ala on the silica TLC, E-PVA-UTLC and AE-PVA-UTLC.

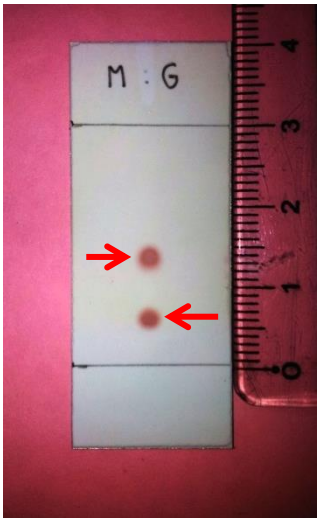
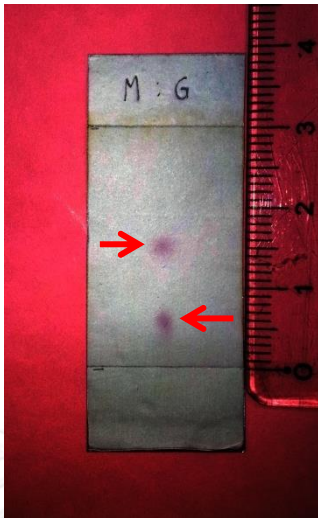
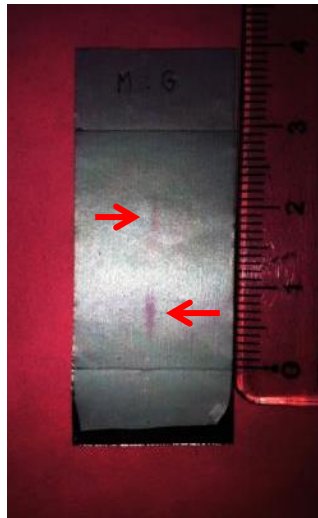
Met (M) : Gln (G)		
Silica TLC	E-PVA-UTLC	AE-PVA-UTLC
		

Figure 4.17 The separation of Met and Gln on the silica TLC, E-PVA-UTLC and AE-PVA-UTLC.

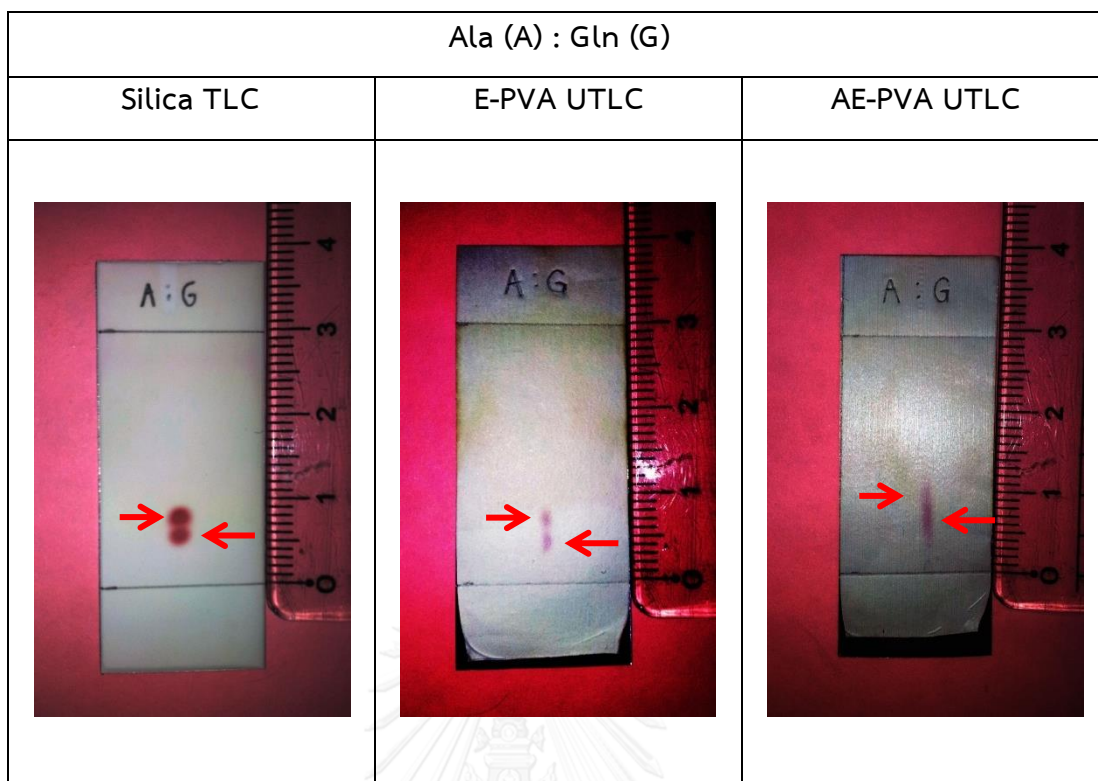


Figure 4.18 The separation of Ala and Gln on the silica TLC, E-PVA-UTLC and AE-PVA-UTLC.

CHAPTER V

CONCLUSION

PVA nanofibers were prepared by crosslinking PVA with glutaraldehyde via electrospinning technique. FT-IR was used to characterize the functional group of crosslinked PVA nanofibers. The crosslinked PVA was achieved as the decreasing in absorbance at 3302 cm^{-1} related to O-H stretching and increasing in absorbance at 1015 cm^{-1} due to C-O-C groups were observed. The morphology was characterized by scanning electron microscopy (SEM). The nanofibers were smooth which diameter was in range of 440-540 nm. The average diameter of AE-PVA was smaller than E-PVA because of the extension by drawing. At same rotational speed, when collector distance was increased, the diameter of nanofibers was slightly decreased. Moreover, rotational speed of the collector affected the alignment of nanofibers. At same collector distance, the alignment of nanofibers increased when rotational speed increased. However, the high rotational speed, 1500 rpm, alignment was decreased because fibers jet might be broken and nanofibers were discontinuous. The satisfied morphology and the highest alignment of electrospun nanofibers were achieved at 1250 rpm of rotational speed and 15 cm of collector distance.

AE-PVA-UTLC and E-PVA-UTLC were applied as the stationary phase in UTLC. The transport of mobile phase was mainly based on capillary flow through porous media. The velocity constant (**K**) of AE-PVA UTLC was $0.0985\text{ cm}^2/\text{s}$ which was twice higher than that of E-PVA and 6 times higher than that of silica fibers UTLC. The velocity constant increased as the increased of rotational speed which corresponding to the alignment of nanofibers and decreased as the increased of collector distance. The velocity constant of AE-PVA plate at 15 cm of collector distance was faster than AE-PVA plate at 20 cm of collector distance and silica TLC. For separation of amino acids, AE-PVA-UTLC can analyzed the studied amino acids. The plate numbers of AE-

PVA-UTLC were 1.1-2.1 times lower than those of silica TLC and 1.2-3.3 times lower than those of E-PVA. Because the spot of AE-PVA-UTLC was oval. When developing progress, the spot was extended that caused efficiency to be lower than E-PVA-UTLC and silica TLC. However, the separations of mixed amino acids were satisfied and comparable with E-PVA-UTLC and silica TLC. Moreover, AE-PVA-UTLC provided 4.5-5 times shorter analysis time compared to E-PVA-UTLC and silica TLC.



REFERENCES

- [1] Mennickent, S., de Diego, M., and Vega, M. Ultrathin-layer chromatography (UTLC). Chromatographia 76(19-20) (2013): 1233-1238.
- [2] Poole, C.F. Chapter 6 - Thin-Layer Chromatography. in Poole, C.F. (ed.)The essence of chromatography, pp. 499-567. Amsterdam: Elsevier Science, 2003.
- [3] Patel, R., Gopani, M., and Patel, M. UTLC: An advanced technique in planar chromatography. Chromatographia 76(19-20) (2013): 1225-1231.
- [4] Beilke, M.C., Zewe, J.W., Clark, J.E., and Olesik, S.V. Aligned electrospun nanofibers for ultra-thin layer chromatography. Analytica Chimica Acta 761 (2013): 201-208.
- [5] Spangenberg, B., Poole, C., and Weins, C. The stationary phase in thin-layer chromatography. Quantitative Thin-Layer Chromatography. Springer Berlin Heidelberg, 2011.
- [6] Bakry, R., Bonn, G.K., Mair, D., and Svec, F. Monolithic porous polymer layer for the separation of peptides and proteins using thin-layer chromatography coupled with MALDI-TOF-MS. Analytical Chemistry 79(2) (2007): 486-493.
- [7] Frolova, A.M., Konovalova, O.Y., Loginova, L.P., Bulgakova, A.V., and Boichenko, A.P. Thin-layer chromatographic plates with monolithic layer of silica: Production, physical-chemical characteristics, separation capabilities. Journal of Separation Science 34(16-17) (2011): 2352-2361.
- [8] Lu, T. and Olesik, S.V. Electrospun polyvinyl alcohol ultra-thin layer chromatography of amino acids. Journal of Chromatography B 912 (2013): 98-104.
- [9] Oko, A.J., Jim, S.R., Taschuk, M.T., and Brett, M.J. Analyte migration in anisotropic nanostructured ultrathin-layer chromatography media. Journal of Chromatography A 1218(19) (2011): 2661-2667.
- [10] Jim, S.R., Taschuk, M.T., Morlock, G.E., Bezuidenhout, L.W., Schwack, W., and Brett, M.J. Engineered anisotropic microstructures for ultrathin-layer chromatography. Analytical Chemistry 82(12) (2010): 5349-5356.

- [11] Clark, J.E. and Olesik, S.V. Technique for ultrathin layer chromatography using an electrospun, nanofibrous stationary phase. Analytical Chemistry 81(10) (2009): 4121-4129.
- [12] Tidjarat, S., Winotapun, W., Opanasopit, P., Ngawhirunpat, T., and Rojanarata, T. Uniaxially aligned electrospun cellulose acetate nanofibers for thin layer chromatographic screening of hydroquinone and retinoic acid adulterated in cosmetics. Journal of Chromatography A 1367 (2014): 141-147.
- [13] Newsome, T.E. and Olesik, S.V. Silica-based nanofibers for electrospun ultrathin layer chromatography. Journal of Chromatography A 1364(0) (2014): 261-270.
- [14] Lee, J. and Deng, Y. Increased mechanical properties of aligned and isotropic electrospun PVA nanofiber webs by cellulose nanowhisker reinforcement. Macromolecular Research 20(1) (2012): 76-83.
- [15] Newsome, T.E. and Olesik, S.V. Electrospinning silica/polyvinylpyrrolidone composite nanofibers. Journal of Applied Polymer Science 131(21) (2014): 40966.
- [16] Smith, R.M. Chapter 2 Column liquid chromatography. Journal of Chromatography Library, ed. Heftmann, E. Vol. Volume 69: Elsevier, 2004.
- [17] Bolto, B., Tran, T., Hoang, M., and Xie, Z. Crosslinked poly(vinyl alcohol) membranes. Progress in Polymer Science 34(9) (2009): 969-981.
- [18] Park, K.E., Jung, S.Y., Lee, S.J., Min, B.-M., and Park, W.H. Biomimetic nanofibrous scaffolds: Preparation and characterization of chitin/silk fibroin blend nanofibers. International Journal of Biological Macromolecules 38(3-5) (2006): 165-173.
- [19] Li, M., Mondrinos, M.J., Gandhi, M.R., Ko, F.K., Weiss, A.S., and Lelkes, P.I. Electrospun protein fibers as matrices for tissue engineering. Biomaterials 26(30) (2005): 5999-6008.
- [20] Rho, K.S., et al. Electrospinning of collagen nanofibers: Effects on the behavior of normal human keratinocytes and early-stage wound healing. Biomaterials 27(8) (2006): 1452-1461.

- [21] Min, B.-M., Lee, G., Kim, S.H., Nam, Y.S., Lee, T.S., and Park, W.H. Electrospinning of silk fibroin nanofibers and its effect on the adhesion and spreading of normal human keratinocytes and fibroblasts in vitro. Biomaterials 25(7–8) (2004): 1289-1297.
- [22] Kenawy, E.-R., et al. Release of tetracycline hydrochloride from electrospun poly(ethylene-co-vinylacetate), poly(lactic acid), and a blend. Journal of Controlled Release 81(1–2) (2002): 57-64.
- [23] Kim, K., et al. Incorporation and controlled release of a hydrophilic antibiotic using poly(lactide-co-glycolide)-based electrospun nanofibrous scaffolds. Journal of Controlled Release 98(1) (2004): 47-56.
- [24] Ahn, Y.C., et al. Development of high efficiency nanofilters made of nanofibers. Current Applied Physics 6(6) (2006): 1030-1035.
- [25] Tsai, P.P., Schreuder-Gibson, H., and Gibson, P. Different electrostatic methods for making electret filters. Journal of Electrostatics 54(3–4) (2002): 333-341.
- [26] Wang, X., Drew, C., Lee, S.-H., Senecal, K.J., Kumar, J., and Samuelson, L.A. Electrospun nanofibrous membranes for highly sensitive optical sensors. Nano Letters 2(11) (2002): 1273-1275.
- [27] Gibson, P.W., Schreuder-Gibson, H.L., and Rivin, D. Electrospun fiber mats: Transport properties. AIChE Journal 45(1) (1999): 190-195.
- [28] Choi, S.W., Jo, S.M., Lee, W.S., and Kim, Y.R. An electrospun poly(vinylidene fluoride) nanofibrous membrane and its battery applications. Advanced Materials 15(23) (2003): 2027-2032.
- [29] Ye, P., Xu, Z.-K., Wu, J., Innocent, C., and Seta, P. Nanofibrous membranes containing reactive groups: electrospinning from poly(acrylonitrile-co-maleic acid) for lipase immobilization. Macromolecules 39(3) (2006): 1041-1045.
- [30] Kaur, S., Kotaki, M., Ma, Z., Gopal, R., Ramakrishna, S., and Ng, S.C. Oligosaccharide Functionalized Nanofibrous Membrane. International Journal of Nanoscience 05(01) (2006): 1-11.
- [31] Ma, Z. and Ramakrishna, S. Electrospun regenerated cellulose nanofiber affinity membrane functionalized with protein A/G for IgG purification. Journal of Membrane Science 319(1–2) (2008): 23-28.

- [32] Jiang, T., Carbone, E.J., Lo, K.W.H., and Laurencin, C.T. Electrospinning of polymer nanofibers for tissue regeneration. Progress in Polymer Science 46(0) (2015): 1-24.
- [33] Huang, Z.-M., Zhang, Y.Z., Kotaki, M., and Ramakrishna, S. A review on polymer nanofibers by electrospinning and their applications in nanocomposites. Composites Science and Technology 63(15) (2003): 2223-2253.
- [34] Baji, A., Mai, Y.-W., Wong, S.-C., Abtahi, M., and Chen, P. Electrospinning of polymer nanofibers: Effects on oriented morphology, structures and tensile properties. Composites Science and Technology 70(5) (2010): 703-718.
- [35] Li, Z. and Wang, C. Electrospun fibers properties. in One-Dimensional nanostructures, pp. 29-73: Springer Berlin Heidelberg, 2013.
- [36] Bhardwaj, N. and Kundu, S.C. Electrospinning: A fascinating fiber fabrication technique. Biotechnology Advances 28(3) (2010): 325-347.
- [37] Eda, G. and Shivkumar, S. Bead-to-fiber transition in electrospun polystyrene. Journal of Applied Polymer Science 106(1) (2007): 475-487.
- [38] Yang, Q., et al. Influence of solvents on the formation of ultrathin uniform poly(vinyl pyrrolidone) nanofibers with electrospinning. Journal of Polymer Science Part B: Polymer Physics 42(20) (2004): 3721-3726.
- [39] Koski, A., Yim, K., and Shivkumar, S. Effect of molecular weight on fibrous PVA produced by electrospinning. Materials Letters 58(3-4) (2004): 493-497.
- [40] Yuan, X., Zhang, Y., Dong, C., and Sheng, J. Morphology of ultrafine polysulfone fibers prepared by electrospinning. Polymer International 53(11) (2004): 1704-1710.
- [41] Supaphol, P. and Chuangchote, S. On the electrospinning of poly(vinyl alcohol) nanofiber mats: A revisit. Journal of Applied Polymer Science 108(2) (2008): 969-978.
- [42] Kenawy, E.-R., et al. Electrospinning of poly(ethylene-co-vinyl alcohol) fibers. Biomaterials 24(6) (2003): 907-913.
- [43] Wei, Q., Tao, D., and Xu, Y. 1 - Nanofibers: principles and manufacture. Functional Nanofibers and their Applications, ed. Wei, Q.: Woodhead Publishing, 2012.

- [44] Casper, C.L., Stephens, J.S., Tassi, N.G., Chase, D.B., and Rabolt, J.F. Controlling surface morphology of electrospun polystyrene fibers: effect of humidity and molecular weight in the electrospinning process. Macromolecules 37(2) (2004): 573-578.
- [45] Baker, M.I., Walsh, S.P., Schwartz, Z., and Boyan, B.D. A review of polyvinyl alcohol and its uses in cartilage and orthopedic applications. Journal of Biomedical Materials Research Part B: Applied Biomaterials 100B(5) (2012): 1451-1457.
- [46] DeMerlis, C.C. and Schoneker, D.R. Review of the oral toxicity of polyvinyl alcohol (PVA). Food and Chemical Toxicology 41(3) (2003): 319-326.
- [47] Chen, C.T., Chang, Y.J., Chen, M.C., and Tobolsky, A.V. Formalized poly(vinyl alcohol) membranes for reverse osmosis. Journal of Applied Polymer Science 17(3) (1973): 789-796.
- [48] Durmaz-Hilmioglu, N., Yildirim, A.E., Sakaoglu, A.S., and Tulbentci, S. Acetic acid dehydration by pervaporation. Chemical Engineering and Processing: Process Intensification 40(3) (2001): 263-267.
- [49] S, P. and R, S. Chemically Resistant Asymmetric Membranes Made from PVA for the Separation of Organic Solvents and Phenols from Aqueous Solutions. Synthetic Membranes: Volume II. Vol. 154: AMERICAN CHEMICAL SOCIETY, 1981.
- [50] Kim, K.-J., Lee, S.-B., and Han, N.W. Effects of the degree of crosslinking on properties of poly(vinyl alcohol) membranes. Polymer Journal 25(12) (1993): 1295-1302.
- [51] Tang, C., Saquing, C.D., Harding, J.R., and Khan, S.A. In situ cross-linking of electrospun poly(vinyl alcohol) nanofibers. Macromolecules 43(2) (2010): 630-637.
- [52] Lang, K., Sourirajan, S., Matsuura, T., and Chowdhury, G. A study on the preparation of polyvinyl alcohol thin-film composite membranes and reverse osmosis testing. Desalination 104(3) (1996): 185-196.

- [53] Huang, R.Y.M. and Rhim, J.W. Modification of poly(vinyl alcohol) using maleic acid and its application to the separation of acetic acid-water mixtures by the pervaporation technique. Polymer International 30(1) (1993): 129-135.
- [54] Yang, E., Qin, X., and Wang, S. Electrospun crosslinked polyvinyl alcohol membrane. Materials Letters 62(20) (2008): 3555-3557.
- [55] Peters, T.A., Poeth, C.H.S., Benes, N.E., Buijs, H.C.W.M., Vercauteren, F.F., and Keurentjes, J.T.F. Ceramic-supported thin PVA pervaporation membranes combining high flux and high selectivity; contradicting the flux-selectivity paradigm. Journal of Membrane Science 276(1-2) (2006): 42-50.
- [56] Martens, P. and Anseth, K.S. Characterization of hydrogels formed from acrylate modified poly(vinyl alcohol) macromers. Polymer 41(21) (2000): 7715-7722.
- [57] Wang, X., Chen, X., Yoon, K., Fang, D., Hsiao, B.S., and Chu, B. High flux filtration medium based on nanofibrous substrate with hydrophilic nanocomposite coating. Environmental Science & Technology 39(19) (2005): 7684-7691.
- [58] Wang, Y. and Hsieh, Y.L. Immobilization of lipase enzyme in polyvinyl alcohol (PVA) nanofibrous membranes. Journal of Membrane Science 309(1-2) (2008): 73-81.
- [59] Hahn-Deinstrop, E. Solvent Systems, Developing Chambers and Development. Applied Thin-Layer Chromatography. Wiley-VCH Verlag GmbH & Co. KGaA, 2007.
- [60] Joseph, S. Basic TLC Techniques, Materials, and Apparatus. in Handbook of Thin-Layer Chromatography: CRC Press, 2003.
- [61] Hyder, M.N., Huang, R.Y.M., and Chen, P. Correlation of physicochemical characteristics with pervaporation performance of poly(vinyl alcohol) membranes. Journal of Membrane Science 283(1-2) (2006): 281-290.
- [62] Figueiredo, K.C.S., Alves, T.L.M., and Borges, C.P. Poly(vinyl alcohol) films crosslinked by glutaraldehyde under mild conditions. Journal of Applied Polymer Science 111(6) (2009): 3074-3080.

- [63] Reis, E.F.d., et al. Synthesis and characterization of poly (vinyl alcohol) hydrogels and hybrids for rMPB70 protein adsorption. Materials Research 9 (2006): 185-191.
- [64] Kanjanaknthon, S. Preparation of titanium dioxide fibers as stationary phase in thin layer chromatography. Master's Degree Program in Petrochemistry and Polymer Science Chulalongkorn University, 2011.





APPENDIX

จุฬาลงกรณ์มหาวิทยาลัย
CHULALONGKORN UNIVERSITY

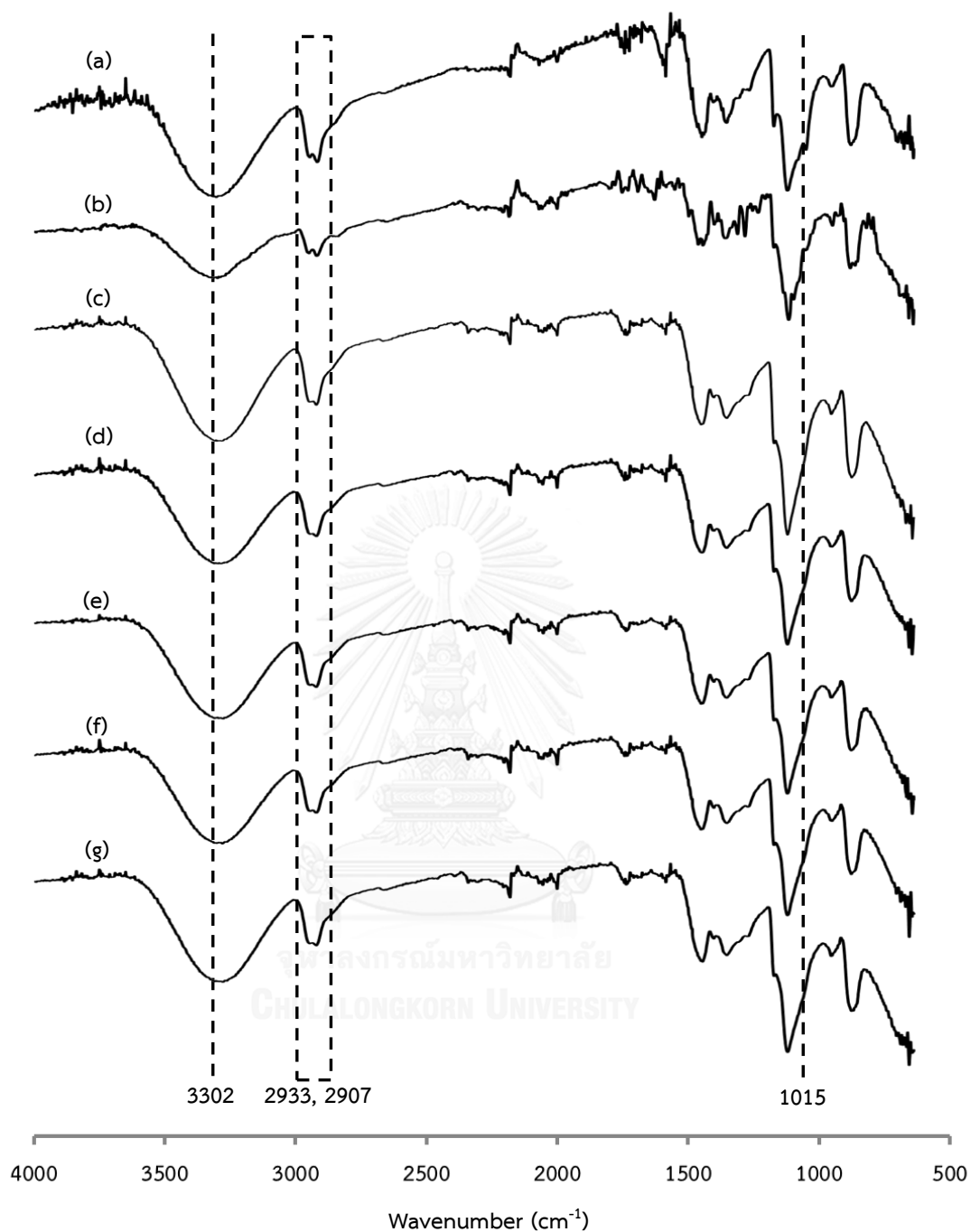


Figure A-1 FT-IR spectra of PVA and crosslinked PVA of 20 cm collector distance. (a) native PVA, (b) E-PVA, (c) AE-PVA at 500 rpm, (d) AE-PVA at 750 rpm, (e) AE-PVA at 1000 rpm, (f) AE-PVA at 1250 rpm and (g) AE-PVA at 1500 rpm.

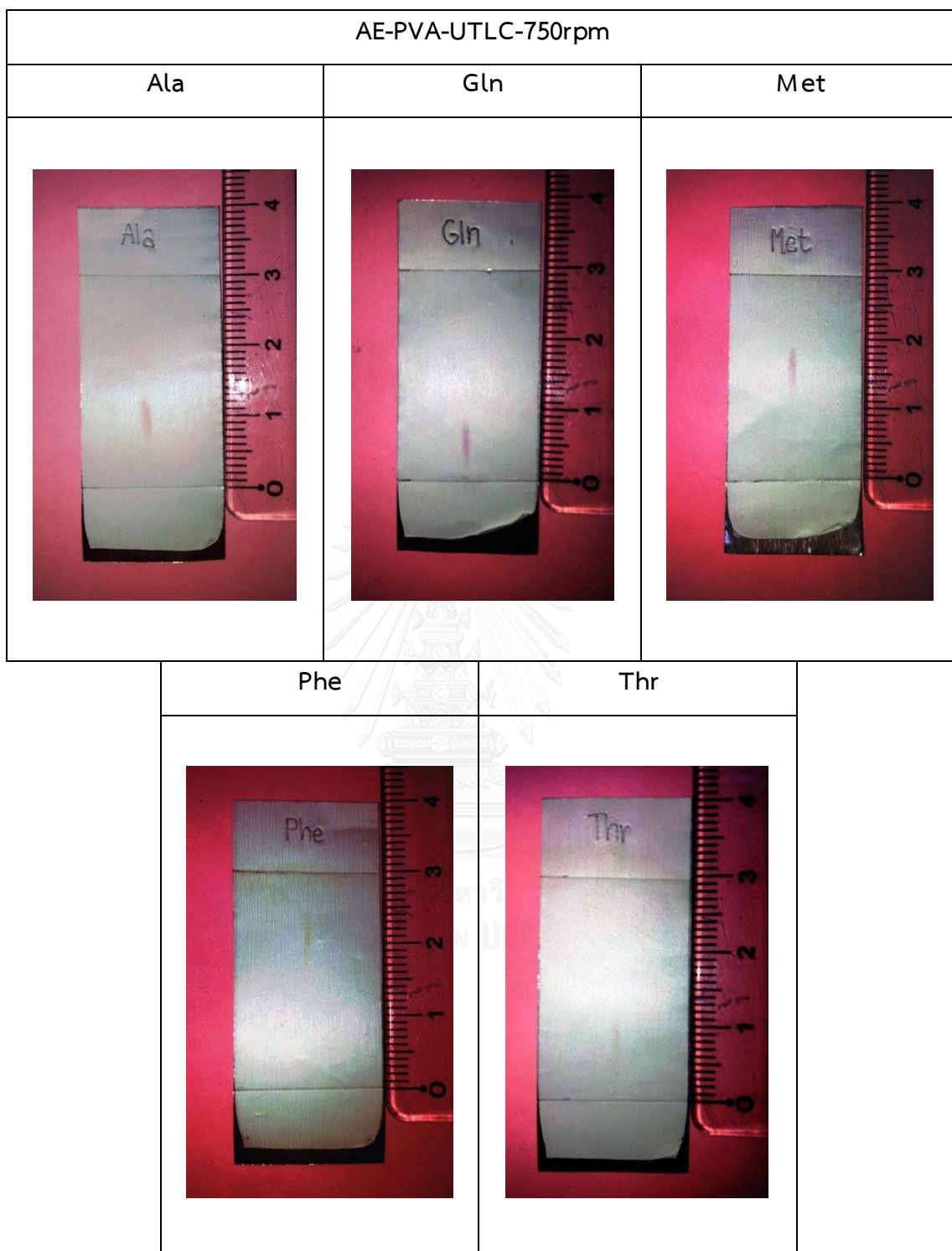


Figure A-2 The analysis of amino acids on the AE-PVA-UTLC at 750 rpm.

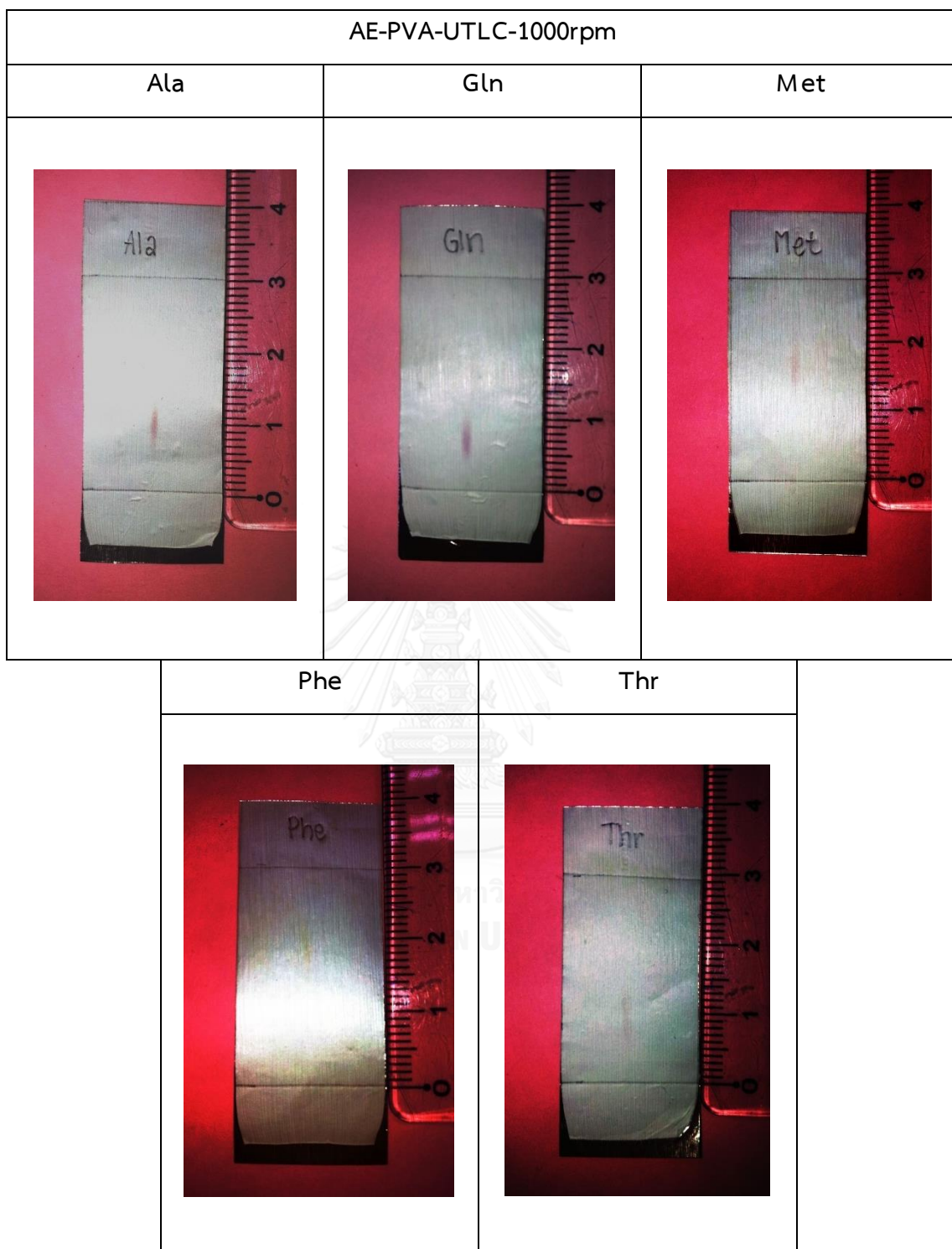


Figure A-3 The analysis of amino acids on the AE-PVA-UTLC at 1000 rpm.

VITA

Miss Waranya Akahardsri was born on February 25, 1989 in Maha Sarakham, Thailand. She graduated with a Bachelor of Science degree in Chulalongkorn University in 2011. After that, she has been a graduate student at the Program of Petrochemistry and Polymer Science, Chulalongkorn University and become a member of Chromatography and Separation Research Unit. She finished her Master's degree of Science in 2015.

Poster presentation and proceeding

“ALIGNED ELECTROSPUN POLY(VINYL ALCOHOL) NANOFIBERS FOR ULTRATHIN LAYER CHROMATOGRAPHY” Waranya Akahardsri and Puttaruksa Varanusupakul. Poster presentation and proceeding, Pure and Applied Chemistry International Conference 2015 (PACCON 2015), Amari Watergate Hotel, Bangkok, Thailand, 21-23 January, 2015.